博士學位論文

Subcritical Water Extraction and Hydrolysis of Citrus Flavonoids: Kinetics, Optimization, and Biological Activities

濟州大學校 大學院

食品工學科

金 東 信

2020年 8月

Subcritical Water Extraction and Hydrolysis of Citrus Flavonoids: Kinetics, Optimization, and Biological Activities

指導敎授 任 尙 彬

金 東 信

이 論文을 工學 博士學位 論文으로 提出함

2020年 8月

金東信의 工學 博士學位 論文을 認准함

審査委員長 金 賢 貞 印
委 員 高 榮 煥 印
委 員 朴 恩 珍 印
委 員 吳 明 哲 印
委 員 任 尙 彬 印

濟州大學校 大學院

2020年 8月

Subcritical Water Extraction and Hydrolysis of Citrus Flavonoids: Kinetics, Optimization, and Biological Activities

Dong-Shin Kim
(Supervised by professor Sang-Bin Lim)

A thesis submitted in partial fulfillment of the requirement for the degree of Doctor of Engineering

2020. 08.

This thesis has been examined and approved.

Hyun Jung Kim, Thesis director, Prof. of Food Science and Engineering

Young Hwan Ko, Prof. of Food Science and Engineering

Eun-Jin Park, Prof. of Food Science and Engineering

Myung-Cheol Oh, Prof. of Food Science and Food Service, Jeju International University

Sang-Bin Lim, Prof. of Food Science and Engineering

Aug. 2020

Department of Food Science and Engineering

GRADUATE SCHOOL

JEJU NATIONAL UNIVERSITY

Contents

Part. Ⅲ. Subcritical Water Extraction and Hydrolysis of Flavonoids from Immature *Citrus unshiu* pomace

1. Materials and Methods

2. Results and Discussion

Abstract

Citrus peels are the main source of many important flavonoids, flavanones (hesperidin and narirutin) and polymethoxyflavones (PMFs; sinensetin, nobiletin, and tangeretin), which have antioxidant, anti-inflammatory, anticancer, and cardioprotective properties. In part 1, the mechanisms controlling the extraction rates of flavonoids from *Citrus unshiu* peel using subcritical water (SW) were studied at different temperatures (120－180 °C) and flow rates (1.0－2.0 mL/min). The extraction yields increased from 40.9, 69.0, and 67.4% at 120 °C to 79.6, 81.9, and 89.0% at 160 °C for hesperidin, narirutin, and PMFs, respectively, while decomposition occurred at 180 °C. The extraction rate curves at different flow rates were used to determine whether the extraction was best described by a thermodynamic partitioning or kinetic desorption model. The extraction rate curves showed that the initial extraction phase is fast, while the subsequent phase is slow. The thermodynamic partitioning model did not match with the experimental data for the latter part of the extraction period. The two-site kinetic desorption model fits the entire extraction period very well, suggesting that the extraction of citrus flavonoids was mainly controlled by intra-particle diffusion. Interestingly, this model fits well even at the pyrolysis temperature (180 °C). Therefore, the two-site kinetic model well described both the decomposition and extraction mechanism of citrus flavonoids when using SW. The diffusion coefficient of hesperidin increased about 9.8-fold at 160 °C and 2 mL/min relative to 120 °C and 1 mL/min. The activation energy of hesperidin (37.2－43.8 kJ/mol) was higher than those of narirutin and PMFs (8.2－36.8 kJ/mol). The use of small amounts of SW, an environmentally friendly solvent, promotes good recovery of flavonoids from citrus peel in a short time.

In part 2, citrus flavonoids were extracted and hydrolyzed from *Citrus unshiu* peel using SW. The individual flavonoid yields, antioxidant and enzyme inhibitory activities of the SW extracts were analyzed. The extraction yields of hesperidin and

narirutin increased with increasing temperature from 145 °C to 165 °C. Hydrothermal hydrolysis products (HHP), such as monoglucosides (hesperetin-7-O-glucoside and prunin) and aglycones (hesperetin and naringenin) were obtained in the SW extracts at temperatures above 160 °C. The sum of hesperidin and its HHP in the SW extracts was strongly correlated with antioxidant activities, whereas the contents of hesperetin and naringenin were strongly correlated with enzyme inhibitory activities. Hesperetin exhibited the highest antioxidant activities (2,2-diphenyl-1-picrylhydrazyl radical scavenging activity, ferric-reducing antioxidant power, and oxygen radical absorbance capacity), whereas hesperetin-7-O-glucoside exhibited the highest enzyme inhibitory activities (angiotensin-Iconverting enzyme (ACE) and pancreatic lipase (PL)). Naringenin exhibited the highest enzyme inhibitory activities (xanthine oxidase and α-glucosidase). PMFs (sinensetin, nobiletin, and tangeretin) also exhibited relatively high inhibitory activities against ACE and PL. This result confirms the potential of SW for extracting and hydrolyzing bioactive flavonoids from *Citrus unshiu* peel.

In part 3, hesperidin was converted into hesperetin-7-O-glucoside and hesperetin with high biological activity in a semi-continuous mode. The optimum condition for maximum production of hesperetin-7-O-glucoside and hesperetin with minimal loss of hesperidin was temperature of 182.8 °C, and residence time of 3.2 min, where the predicted maximum yields of hesperetin-7-O-glucoside and hesperetin were 11,499.5 and 8,030.1 μg/g dry sample, respectively. Temperature was an important factor in SW hydrolysis of hesperidin. The effect of the residence time on hydrolysis was dependent on the temperature, where the short residence time was required at high temperature. This result confirmed the possibility of the conversion of hesperidin to valuable compounds with short time using an environmentally friendly solvent (water).

LIST OF FIGURES

LIST OF TABLES

Introduction

Citrus unshiu is a major fruit grown in Jeju, Korea, and is widely used in the food industry for juice production. As the yield of citrus juice from fresh fruit is approximately 50% of the fruit by weight, large amounts of byproducts, such as peel, pulp, and seeds, are produced (An et al., 2016). Citrus peel represents the major byproduct from the citrus juice industry. Citrus peel has been used to treat the common cold, indigestion, bronchial discomfort, etc., in Korean traditional medicine (Kim et al., 2018a; Kim et al., 2019). Citrus peel is a major source of citrus flavonoids, such as hesperidin, narirutin, and polymethoxyflavones (PMFs; e.g., sinensetin, nobiletin, and tangeretin), which have various functional properties, including antioxidant, antimicrobial, anticancer, anti-inflammatory, antiobesity, or antihyperglycemic activities (Burke et al., 2018; Kim et al., 2018b; Revathy et al., 2018).

The extraction of citrus flavonoids is generally accomplished using organic solvents such as ethanol, methanol, and acetone due to their poor solubility in water (Mehood et al., 2015; Singanusong et al., 2015), but their use is limited by the toxicity of the solvent residue, strict legislation, and long extraction times (Lachos-Perez et al., 2018). Recently, high pressure and ultrasound- assisted extraction methods have been used to increase the extraction efficiency, but it is still not possible to avoid the use of organic solvents (Nipornram et al., 2018).

As an alternative to organic solvent extraction, subcritical water extraction (SWE), an environmentally friendly technique, has been used to extract medium- or non-polar bioactive compounds from plant materials. SW is water that maintains a liquid state at a temperature of 100 °C－374 °C under pressure. In the subcritical region, the dielectric constant associated with the polarity of water is reduced due to the breakdown of hydrogen bonds between the water molecules, which allows the extraction of medium- or non-polar compounds, such as flavonoids (Gbashi et al., 2016). SW also improves extraction efficiency by reducing viscosity and surface

tension, and increasing the self-diffusion of water (Cheigh et al., 2012). Additionally, the subcritical condition increases the levels of ionic products of water, thus forming an acidic medium for hydrolysis reactions (Shitu et al., 2015), and flavonoid diglucosides can be hydrolyzed to flavonoid monoglucosides and aglycones using SW (Fig. 1).

During SWE, the following steps are proposed for transferring target compounds from the sample to the extraction solvent. The solute is desorbed from the original binding site of the sample matrix (internal diffusion), and is then eluted to the extraction solvent (external elusion) (Kubátová et al., 2002; Kim and Mazza, 2007; Asl and Khajenoori, 2013). Depending on the sample matrix and extraction conditions, the initial desorption step or subsequent elution step may control the actual rate of extraction. SWE has been applied to a wide range of plant samples, but little research has been conducted on the fundamental extraction mechanisms for different sample matrices. Investigating these mechanisms via partitioning thermodynamics and desorption kinetics could improving our understanding thereof. This would provide information useful for assessing the possible scale and economics of new devices for commercial production (Anekpankul et al., 2007).

There have been several studies on the extraction of phenolic compounds from *Citrus unshiu* using SW over the past decade. Cheigh et al. (2012) studied the SWE of hesperidin and narirutin from citrus fruits by varying extraction temperature (110 °C－200 °C) and static time (5－20 min) in batch mode. Kanmaz and Saral (2017) extracted mandarin peel using SW and determined the effects of extraction temperature (50 °C－180 °C) and static time (5 and 15 min) on total phenolic and flavonoid contents and the antioxidant activities of the SW extracts in batch mode. Lachos-Perez et al. (2018) studied the effects of extraction temperature (110 °C－150 °C) and flow rate (10－30 mL/min) on flavonoid yields from defatted orange peel using a semi-continuous SWE unit. However, to date, no kinetic modeling studies of the extraction of bioflavonoids from *Citrus unshiu* peel have been performed, and most studies reported to date conducted only single-factor experiments on extraction

temperature and static time mainly using a batch-type extractor. In addition, various functionalities of the SW extracts and hydrolysates from *Citrus unshiu* peel have not been measured, and there have been no studies regarding which chemical compounds determine the functional properties of the SW extracts and hydrolysates.

The objectives of this study are as follows; Part 1: The mechanism controlling the extraction rates of representative flavonoids from citrus peel using SW was investigated. The relative importance of internal desorption and external elution was analyzed under different flow rates. The extraction kinetics were determined by fitting the experimental data to thermodynamic partitioning and two-site kinetic desorption models. In addition, the diffusion coefficients and activation energies of citrus flavonoids during SWE were also evaluated. Part 2: the extraction parameters (extraction temperature and flow rate) were optimized using response surface methodology (RSM) to maximize the yields of five flavonoids, i.e., hesperidin, narirutin, sinensetin, nobiletin, and tangeretin, from *Citrus unshiu* peel using SW. Functional properties, such as the antioxidant activities (2,2-diphenyl-1-picrylhydrazyl [DPPH] radical scavenging activity, ferric-reducing antioxidant power (FRAP), and oxygen radical absorbance capacity (ORAC)) and enzyme inhibitory activities (against xanthine oxidase (XO), angiotensin-I converting enzyme (ACE), α-glucosidase, and pancreatic lipase (PL)) of the SW extracts and individual citrus flavonoids, including their hydrolysis products, were also analyzed. Part 3: Subcritical water extraction of hesperidin and narirutin from immature *Citrus unshiu* pomace was optimized. In addition, hydrolysis parameters (temperature and residence time) were optimized to maximize the conversion yields of hesperetin-7-O-glucoside and hesperetin with high biological activities from subcritical water extract.

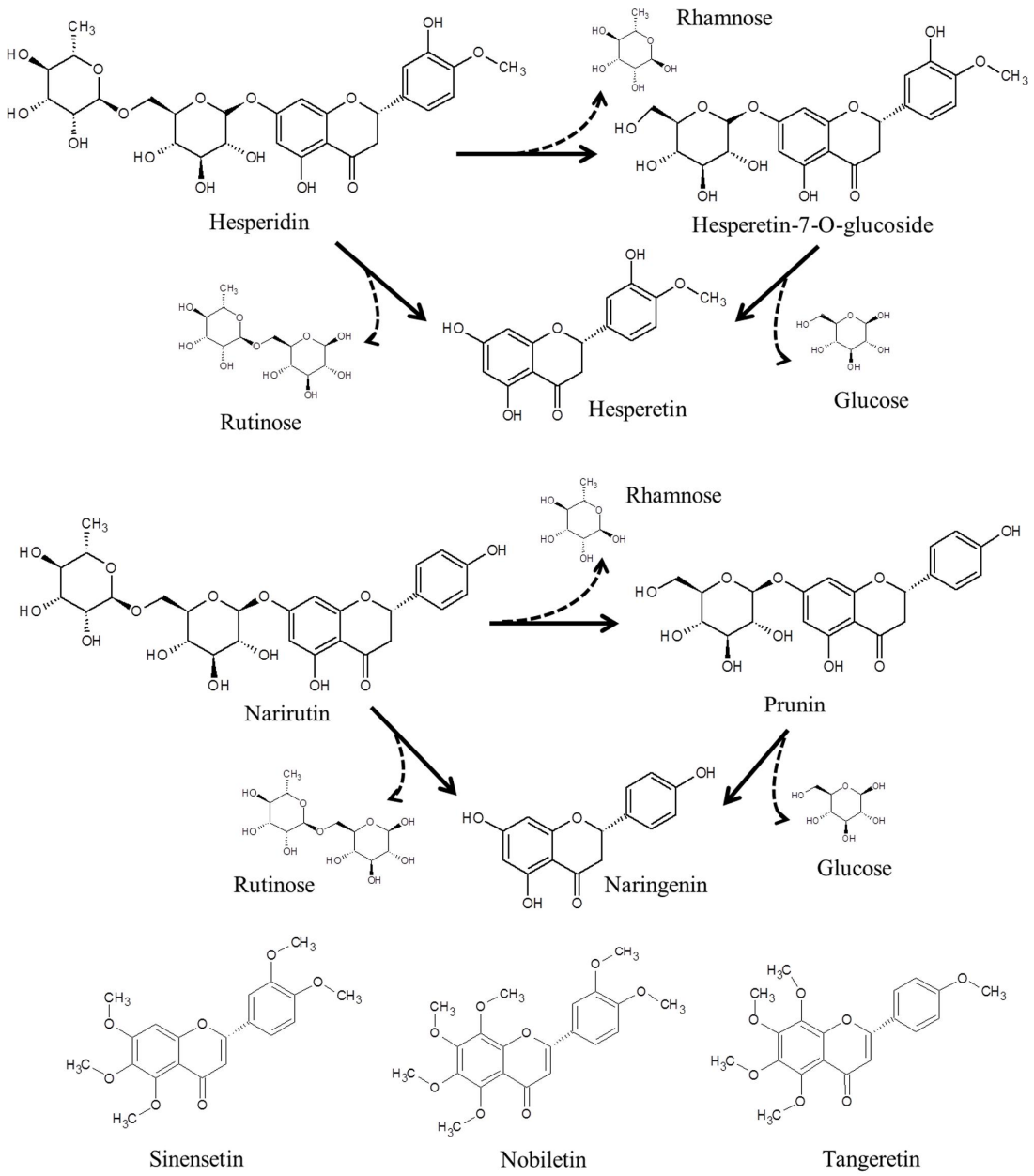

Fig. 1. Chemical structures and hydrolysis pathways of citrus flavonoids.

Part. Ⅰ

Kinetic Study of Subcritical Water Extraction of Flavonoids from *Citrus unshiu* peel

1. Materials and Methods

1.1. Samples and chemicals

Citrus peel was separated from *Citrus unshiu* Markovich fruits purchased from a local farm in Jeju, Republic of Korea. The peel was dried in the shade, pulverized using a Waring blender (Waring Products Division, New Hartford, CT, USA), and sieved (mean particle diameter: 575 μm). Approximately 1 g of citrus peel was used for SWE. Hesperidin (94%) and narirutin (99%) were purchased from Sigma Chemical Co. (St. Louis, MO, USA) and sinensetin (98%), nobiletin (98%), and tangeretin (98%) were purchased from Avention (Yeonsu-gu, Incheon, Republic of Korea). High-performance liquid chromatography-grade acetonitrile and methyl alcohol were obtained from Daejung Chemicals (Siheung, Gyeonggi, Republic of Korea) and acetic acid was purchased from Junsei Chemical Co., Ltd. (Tokyo, Japan). Methanol (99.9%) and ethanol (99.8%) were purchased from CARLO ERBA Reagents (Val de Reuil, France), and acetone (99.5%) was from TEDIA (Fair-field, OH, USA).

1.2. Subcritical water extraction

Semi-continuous SWE was performed in our lab-built apparatus (Fig. 2). All extractions of citrus peel were carried out in a stainless steel extractor (7.8 mm × 300 mm, 14 mL) equipped with 5-μm stainless steel frits at both ends. Glass wool was placed at the outlet of the extraction column to prevent clogging of samples. The extractor was filled with the sample (1.0 g), mixed with sea sand (14－20 mesh; Junsei Chemical Co., Ltd., Tokyo, Japan) to avoid sample compaction and mounted vertically in a gas chromatograph oven (HP 5890; Agilent Technologies, Santa Clara, CA, USA) with water flowing from bottom to top. The extraction was started by heating the oven to the required temperature and pressurizing with water to 5 MPa; this process took less than 5 min. A piston pump (Thermo Separation

Products, Waltham, MA, USA) was used to deliver the deionized and degassed water. A back-pressure regulator (Tescom Corp., Elk River, MN, USA) at the outlet of the extraction system was set to 5 MPa to keep water in its liquid state for all of the temperatures studied. The water flow rate was set to the desired rate using a metering valve (Parker Autoclave Engineers, Erie, PA, USA), and the extract collection was thus started. For the analysis of the extraction rate, each fraction was collected every 2 or 5 min for 30 min and was stored in a freezer at −20 °C before analysis.

The content of individual flavonoids in the raw citrus peel was measured by extracting a sample (1.0 g) with 30 mL of methanol for 30 min at room temperature five times, and calculating the average values of three replications.

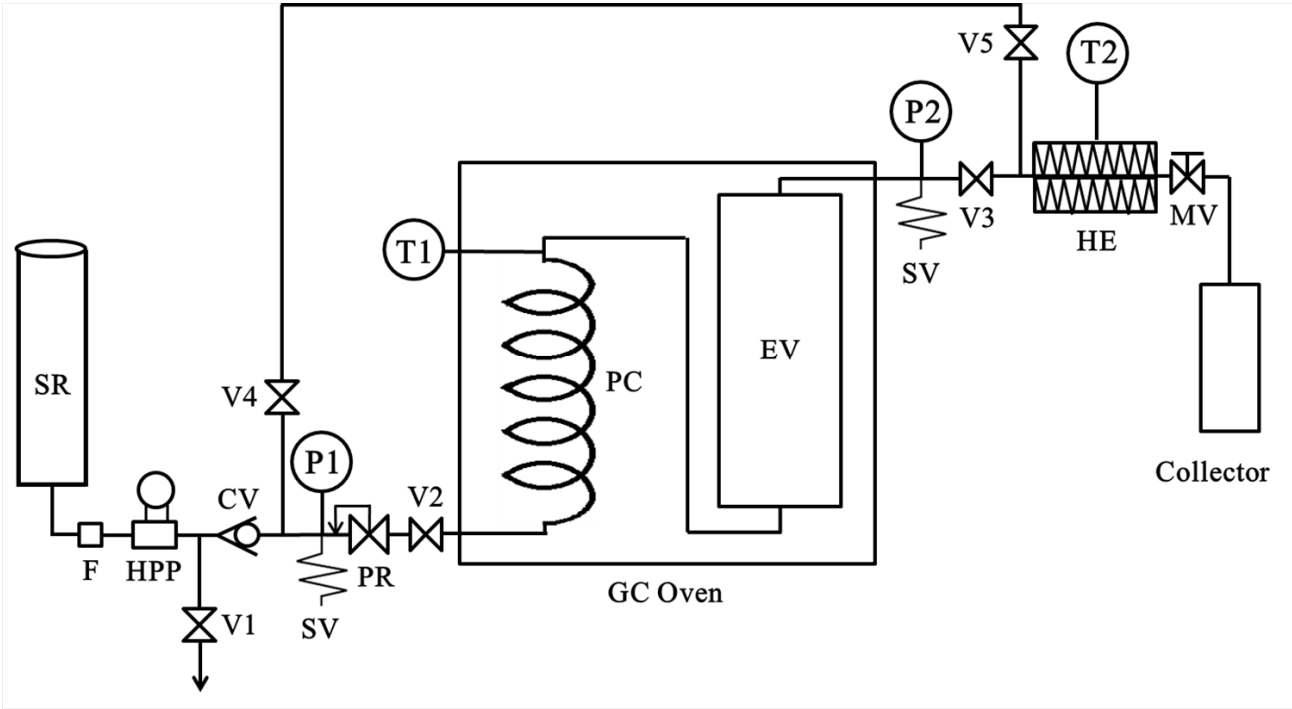

Fig. 2. Schematic diagram of semi-continuous subcritical water extraction apparatus (CV: check valve, EV: extraction vessel, F: in-line filter, HE: heat exchanger, HPP: high pressure pump, MV: metering valve, P: pressure gauge, PC: preheating coil, PR: pressure regulator, SV: safety valve, SR: solvent reservoir, T: temperature indicator, V: on/off valve).

1.3. Conventional organic solvent extraction

For each extraction, one gram of *Citrus unshiu* peel was extracted using 30 mL of methanol, ethanol, and acetone at 65, 78, and 56 °C, respectively. The mixture was shaken at 120 rpm in a water bath (Jeio Tech. Co., Ltd., Daejeon, Republic of Korea) for 15 min and filtered (No. 5A, Advantec Toyo Kaisha, Ltd., Tokyo, Japan). The extracts were adjusted to a specific volume using each solvent and filtered (0.45 μm) before HPLC analysis.

1.4. HPLC analysis

HPLC analysis was carried out for each fraction collected every 2 or 5 min for 30 min in SWE. Quantitative analyses of five flavonoids (narirutin, hesperidin, sinensetin, nobiletin, and tangeretin) in the extracts were performed using a high-performance liquid chromatography system (Alliance 2965; Waters Corp., Milford, MA, USA). Chromatographic separations were accomplished using an Inertsil ODS-3V column (5 μm, 4.6 × 250 mm; GL Science, Tokyo, Japan). Solvent A was 0.1% acetic acid solution and solvent B was acetonitrile. The mobile phase was programmed as follows: 0 min 15% B, 8 min 25% B, 15 min 25% B, 35 min 65% B, 37 min 65% B, and 39 min 15% B. The flow rate was 1.0 mL/min and the column temperature was 40 °C. The injection volume was 10 μL and the detection was performed at wavelengths of 290 and 330 nm. The chromatographic peaks of flavonoids were identified by comparing their UV‐visible spectra and retention times to those of each standard compound, and quantified based on the calibration curves of standard compounds (Amaretti et al., 2015; Kim and Lim, 2019)

1.5. Kinetic modeling

1.5.1. Thermodynamic partitioning model

This model assumes that the internal diffusion of the particles and subsequent partitioning of the solute into the solvent is fast, and that the extraction process is controlled by the thermodynamic equilibrium (Islam et al., 2013). The partition coefficient (K_D) is defined as the ratio of the solute in the sample to that in the solvent at equilibrium after a certain time. The K_D model can be described by:

$$\frac{C_b}{C_0} = \frac{C_a}{C_0} + \frac{1 - C_a/C_0}{1 + K_D m/\rho(V_a - V_b)} \quad (1)$$

where C_0 is the initial solute content (mg/g) in the sample, C_a and C_b are the solute contents (mg/g) extracted from water volumes V_a and V_b (mL), respectively, m is the sample mass (mg), and ρ is the density (mg/mL) of extraction solvent for a given condition. The K_D model only includes the solvent volume; therefore, the extraction rate should increase in proportion to the solvent volume if the extraction is described well by this model.

1.5.2. Two-site kinetic desorption model

The two-site kinetic desorption assumes that the extraction process is governed by the initial desorption step in the sample matrix. This model predicts an extraction curve using fast and slow functions. The solute fraction (F) released quickly is described by the fast desorption rate constant (k_1), while that released slowly ($1 - F$) is described by the slow desorption rate constant (k_2) (Duba et al., 2015). The model is described by two first-order expressions, as follows:

$$\frac{C}{C_0} = 1 - F\exp(-k_1 t) - (1 - F)\exp(-k_2 t) \quad (2)$$

where C_0 is the initial solute content (mg/g) in the sample and C is the solute content (mg/g) extracted after time t (min)

The parameters were calculated by fitting the experimental data at different temperatures (120－180 °C) and flow rates (1－2 mL/min) to each model using Microsoft Excel 2010 Solver (Microsoft Corp., Redmond, WA, USA).

1.6. Statistical analysis

All experimental results are expressed as the mean ± standard deviation of three replications. Significant differences ($p < 0.05$) were determined by Duncan's multiple range test, performed using SPSS software (ver. 18.0; SPSS Inc., Chicago, IL, USA).

2. Results and Discussion

2.1. Composition of flavonoids in *Citrus unshiu* peel

The flavonoid composition in the methanol extract of *Citrus unshiu* peel is shown in Table 1. The major flavonoids were hesperidin (50,027 μg/g dry sample) and narirutin (9,284 μg/g dry sample). Monoglucosides and aglycones other than hesperidin and narirutin were not detected. The minor flavonoids were PMFs (0.3%) such as sinensetin (18.9 μg/ g dry sample), nobiletin (103.8 μg/g dry sample), and tangeretin (55.5 μg/g dry sample). The sum of all flavonoid contents was 59,490 μg/g dry sample.

Table 1. Composition of flavonoids in *Citrus unshiu* peel.

Flavonoid	Content (μg/g dry sample)	(%)
Hesperidin	50,027.4 ± 970.8	84.1
Narirutin	9,284.4 ± 241.1	15.6
Sinensetin	18.9 ± 0.2	0.03
Nobiletin	103.8 ± 0.5	0.18
Tangeretin	55.5 ± 0.3	0.09
Total	59,490.0 ± 1211.5	100

Data are expressed as the mean ± standard deviation of triplicate experiments.

2.2. Effect of extraction temperature

The water temperature greatly affects the performance of SWE in terms of solubility and the mass transfer rate (Plaza and Turner, 2015; Gbashi et al., 2016). The effect of water temperature on the cumulative extraction yields of representative citrus flavonoids was measured in the temperature range of 120−180 °C at 5 MPa at a flow rate of 1.5 mL/min (Fig. 3). The extraction yield (%) was defined as the mass sum (mg) of all flavonoids in the extract of each extraction time divided by that of the dried raw material. At 120 °C, 40.9, 69.0, and 67.4% of hesperidin, narirutin, and PMFs, respectively, were extracted from citrus peel; the amounts increased to 79.6, 81.9, and 89.0%, respectively, when the temperature increased to 160 °C for 30 min. Temperature had a large effect on the hesperidin yield, which was 1.94-fold higher at 160 °C than at 120 °C. Céliz et al. (2014) reported that the solubility of pure hesperidin in water was 2.5 times as high when the temperature increased from 120 to 150 °C. Meanwhile, temperature had a smaller effect on the narirutin yield, which was only 12.9% higher at 160 °C than at 120 °C, because narirutin has a higher solubility in water than hesperidin (Park et al., 2012). In the case of PMFs, even though it has low solubility in water (Lai et al., 2015), the yield was 21.6% higher at 160 °C than at 120 °C.

The higher yield of citrus flavonoids at higher temperatures may be due to the decreased dielectric constant and polarity of water (in turn due to the reduction in polar forces between the water molecules), which makes it more suitable for the extraction of less polar compounds (Plaza and Turner, 2015; Gbashi et al., 2016). Also, as the water temperature rises, the viscosity and surface tension of the water decrease and the diffusivity of water increases, resulting in increased mass transfer rate of the solute from the sample matrix into the solvent (Nastic et al., 2018; Yan et al., 2020). The dielectric constant of water decreases to 50.5 and 41.9 at 120 and 160 °C, respectively, from 80.2 at 20 °C (Bruner, 2014). The viscosity of water decreases to 232×10^{-6} and 170×10^{-6} Pa·s at 120 °C and 160 °C, respectively,

from 1,002 × 10^{-6} Pa·s at 20 °C (Senger and Watson, 1986). The surface tension of water decreases to 56.9 and 48.3 mN/m at 110 °C and 150 °C, respectively, from 72.7 mN/m at 20 °C. The diffusivity of water increases to 9.8 × 10^{-9} and 15.7 × 10^{-9} m^2/s at 110 °C and 150°C, respectively, from 2.3 × 10^{-9} m^2/s at 25 °C (Bruner, 2014).

At 180 °C the yield of flavonoids initially increased, but after 10 min of extraction the yield began to decrease compared to 160 °C. This confirmed that thermal hydrolysis or degradation of flavonoids occurred at a temperature higher than 160 °C. Also, Lachos-Perez et al. (2018) reported that the degradation of hesperidin and narirutin extracted from defatted orange peel using SW started above 160 °C.

It is necessary to ensure that the amount of each flavonoid in the raw material is below its saturation concentration at each water temperature, particularly for hesperidin (because its content in the raw sample is very high). The solubility of pure hesperidin in water (calculated by extrapolation) is ~2,537 mg/L at 160 °C (Céliz et al., 2014). Since the content of hesperidin in the raw sample is 50,027 μg/g dry sample, saturation of water with hesperidin would yield 1,667 mg/L which is substantially below the solubility limit.

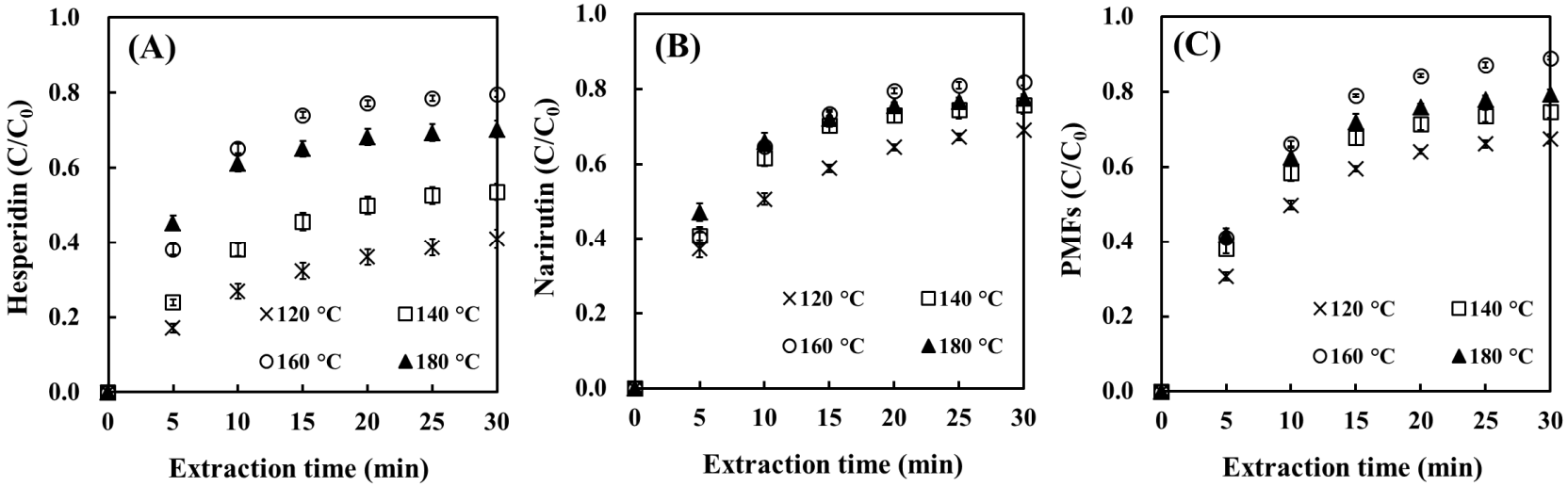

Fig. 3. Effect of water temperature on extraction yields of flavonoids from citrus peel under a water flow rate of 1.5 mL/min (PMFs, polymethoxyflavones).

2.3. Effect of water flow rate

Fig. 4 shows the extraction rate curves generated by SWE of representative flavonoids from citrus peel with flow rates in the range 1－2 mL/min at 160 °C. The extraction rate curves obtained in this study were generally similar to those reported in the literature (Kubátová et al., 2002; Kim and Mazza, 2007; Asl and Kajenoori, 2013; Anekpankul et al., 2007; Ho et al., 2008; Khajenoori and Asl, 2009; Barrera Vázquez et al., 2015; Duba et al., 2015; Kim and Lim, 2019). As shown by the SWE curves, there was an initial extraction phase that was quite fast, followed by a subsequent slow phase. The extraction yields of citrus flavonoids increased from 70.5, 80.6, and 84.1% at 1 mL/min after 30 min to 85.0, 86.3, and 90.7% at 2 mL/min after 15 min for hesperidin, narirutin, and PMFs, respectively, at 160 °C. The yield increased with flow rate due to the increases in the mass transfer rate, superficial velocity, and concentration gradient of the solute between the sample and the solvent during the extraction process (Shabkhiz et al., 2016; Mottahedin et al., 2017). Shabkhiz et al. (2016) reported that the yield of glycyrrhizic acid from licorice root increased with the flow rate at 100－150 °C when SW was used. At a flow rate of 2 mL/min, the yields of all flavonoids reached the highest values after 15 min of extraction. Therefore, when SW was used, the time required to recover flavonoids from citrus peel can be minimized by increasing the flow rate, without diluting the concentration of flavonoid compounds in the final product (Gbashi et al., 2016; Mottahedin et al., 2017).

Whether a particular extraction process is controlled by the K_D model, which depends on the extraction solvent volume, or by the two-site model, which depends on the extraction time, it can be determined based on the effect of different flow rates on the extraction yields of the target compound. Fig. 4 shows that the extraction rates of all flavonoids increased in proportion to the solvent flow rate, regardless of whether extraction was fast (narirutin and PMFs) or slow (hesperidin). All extraction curves showed the behavior expected based on the K_D model; direct

dependence of the extraction yield on flow rate was apparent, particularly in the initial extraction phase. In addition to this behavior consistent with the K_D model, other behaviors expected based on the two-site kinetic desorption model were observed in the extraction curves. That is, once the fast-released fractions were recovered (after ~10 min), the extraction curves of the slowly released fractions became increasingly parallel. However, we cannot draw any definitive conclusions based only on the shapes of the extraction curves in Fig. 4 because, without fitting experimental data to model equations, the relative importance of the K_D and the two-site models cannot be estimated precisely.

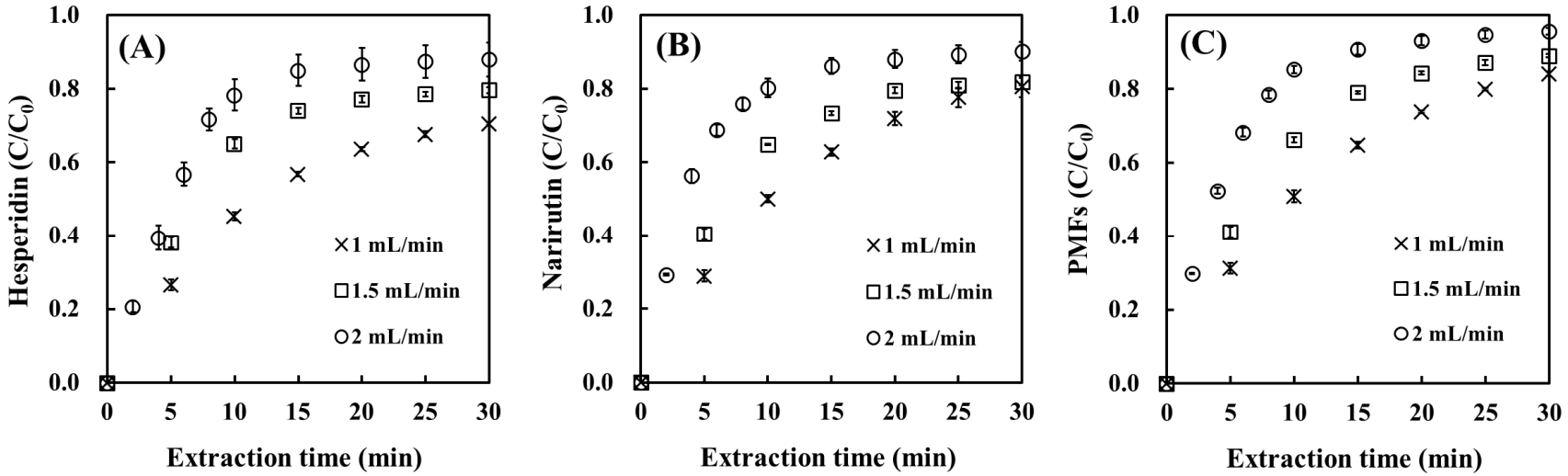

Fig. 4. Effect of water flow rate on subcritical water extraction yields of flavonoids from citrus peel at 160°C (PMFs, polymethoxyflavones).

2.4. Kinetic modeling

2.4.1. Thermodynamic partitioning model

To test the applicability of the thermodynamic partitioning model to the SWE rate curves of citrus flavonoids, The K_D values of each flavonoid were calculated by fitting the experimental data to the K_D model equation (Table 2). As expected, the K_D values obtained under different flow rates at the same temperature were statistically the same. The K_D values of all flavonoids decreased as the temperature increased from 120 to 160 °C. K_D describes the partition of solute between the sample matrix and the extraction solvent during the extraction process; a decrease in K_D with increasing temperature indicates an increase in the extraction efficiency due to weakened competition for the solute between the solvent and the matrix (Asl and Khajenoori, 2013; Islam et al., 2013).

Hesperidin has a wider range of K_D values, from 14.8 to 62.2, compared to narirutin (14.0－23.4) and PMFs (12.1－23.0) at temperatures of 120－160 °C. The K_D value of hesperidin was about 2.7 times higher than that of narirutin at 120 °C. However, as the temperature increased to 160 °C, the K_D value of hesperidin decreased to become comparable to that of narirutin, due to the rapid increase in the solubility of hesperidin in water at 160 °C. Céliz et al. (2014) reported that the solubility of pure hesperidin in water was low (1.33 mM) at 120 °C, but increased about 2.5-fold (3.41 mM) as the temperature increased to 150 °C.

The K_D model was applied to the experimental extraction data of flavonoids from citrus peel (Fig. 5). The K_D model curves did not match well with the experimental data, particularly in their latter parts, and thus were not suitable for describing the extraction behavior over the entire extraction period. The extraction curve showed that the yield tended to increase rapidly in the beginning, and slowly thereafter (after ~10 min). Although the K_D model fit well up to 10 min, it fit poorly thereafter. The slow extraction phase may be attributable to the desorption kinetics. The sample matrix of citrus peel seems to have two sorption sites: one with a fast-release

fraction and the other with a slow-release fraction.

Table 2. Distribution coefficients obtained by curve-fitting the thermodynamic partitioning model to the experimental extraction data for flavonoids when using subcritical water.

Temperature (°C)	Flow rate (mL/min)	Partitioning coefficients (K_D)		
		Hesperidin	Narirutin	PMFs
120	1	61.7 ± 3.3[a]	23.4 ± 0.8[a]	22.0± 1.3[a]
	1.5	62.2 ± 2.6[a]	23.4 ± 1.1[a]	23.0± 1.0[a]
	2	60.8 ± 2.6[a]	22.7 ± 0.8[a]	22.5± 1.8[a]
140	1	29.4 ± 2.1[b]	18.6 ± 1.1[b]	18.6± 0.5[b]
	1.5	30.8 ± 1.1[b]	18.0 ± 0.2[b]	17.2± 0.7[b]
	2	29.8 ± 2.1[b]	18.2 ± 0.4[b]	17.5± 1.3[b]
160	1	15.3 ± 0.3[c]	14.4 ± 0.9[c]	12.2± 0.5[c]
	1.5	15.0 ± 0.7[c]	14.1 ± 0.3[c]	12.3± 0.4[c]
	2	14.8 ± 0.5[c]	14.0 ± 0.3[c]	12.1± 0.3[c]

PMFs (polymethoxyflavones); sinensetin, nobiletin, and tangeretin.

Data are expressed as the mean ± standard deviation of triplicate extractions.

The means in each column followed by the same letter ([a-c]) are not significantly different by Duncan's multiple range test at $p < 0.05$.

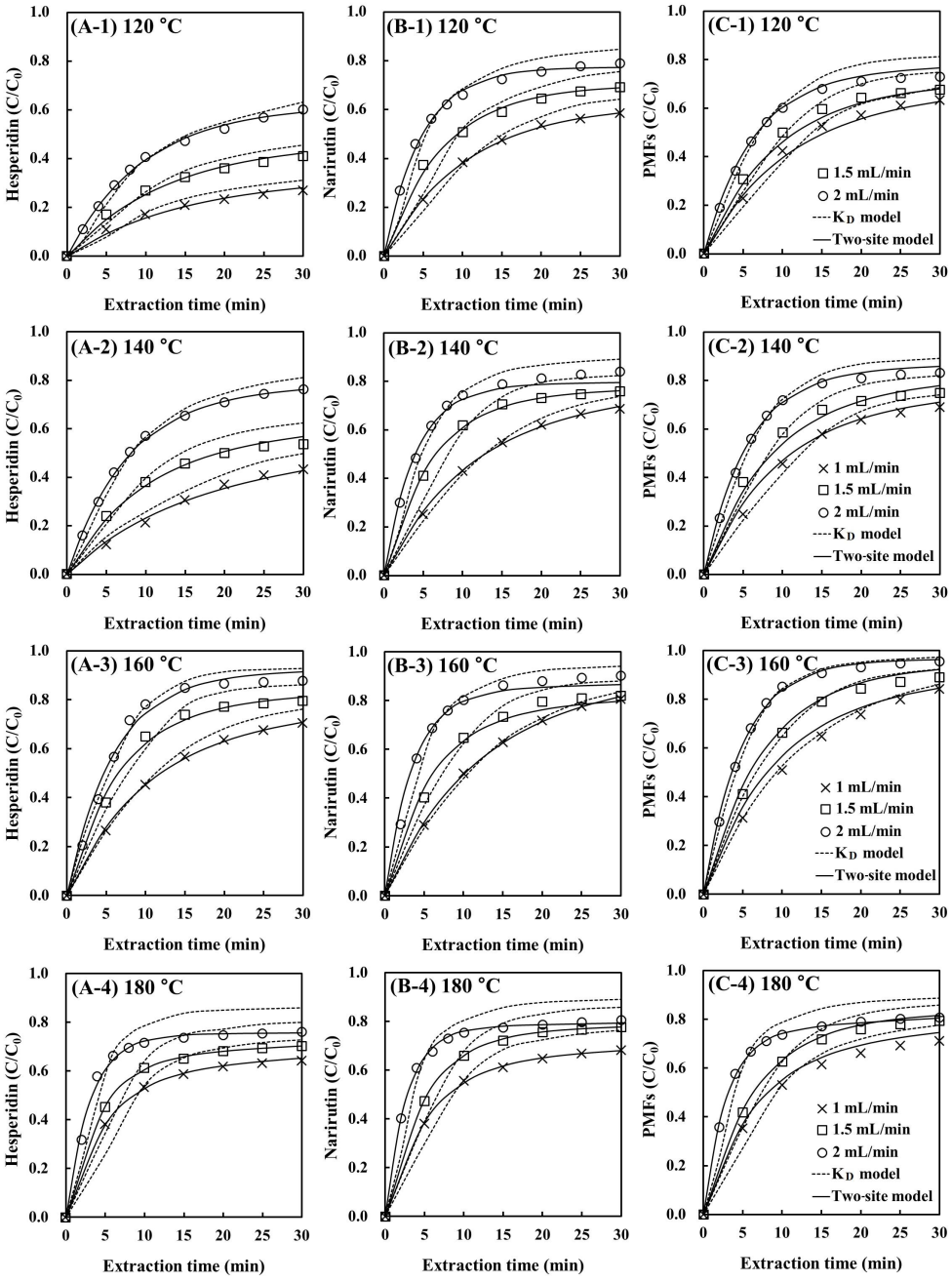

Fig. 5. The fit of the thermodynamic partitioning and two-site kinetic desorption models to experimental data for subcritical water extraction of flavonoids from citrus peel (PMFs). Symbols represent the experimental data and the dotted lines and solid lines are based on the K_D and two-site kinetic desorption model equation, respectively.

2.4.2. Two-site kinetic desorption model

We fitted the two-site kinetic desorption model to the experimental extraction data (Table 3). k_1 for all flavonoids increased with temperature due to the decreased dielectric constant and viscosity of water, and the increased energy for desorption of the solute (Islam et al., 2013; Duba et al., 2015). k_1 also increased with flow rate, because the solutes that reached the surface of the particles were rapidly washed away, and the internal diffusion would be increased by the higher concentration gradient between the interior and exterior of the particles (Kim and Mazza, 2007). k_2 for all flavonoids also increased with temperature, but decreased with increasing flow rate. Kim and Lim (2019) reported that the k_2 value of rutin extracted from buckwheat using SW followed both of these trends. Like k_1, F for all flavonoids increased with temperature and flow rate. Especially, the value of F for hesperidin at 120 °C and 1 mL/min was only 0.297, but increased more than 3-fold (0.904) at 160 °C and 2 mL/min because the solubility of hesperidin in water increased abruptly at 160 °C (Céliz et al., 2014).

Fig. 5 presents the fit of the two-site kinetic desorption model to the SWE data for citrus flavonoids. The fit is very good for the entire extraction period. If the desorption rate of the solute is controlled by the concentration gradient between the sample matrix and the extraction solvent, the extraction rate would increase, especially in the early stages of the extraction process when the solute content of the sample is high. A high flow rate can also cause rapid elution of flavonoids that are released quickly from the sample matrix. Once the “fast” component of the desorption compound had been depleted, the effect of the flow rate lessened, since the rate of desorption of the “slow” component was very low. This resulted in the extraction curves being parallel, without any further increase after 10 min of extraction. Thus, the two-site kinetic model fit very well, according to both the latter half and early part of the extraction curve, compared to the K_D model.

Table 3. The values of the parameters F, k_1 and k_2 obtained by curve-fitting the two-site kinetic model to the experimental data for flavonoids when using subcritical water.

Temperature (°C)	Flow rate (mL/min)	Hesperidin			Narirutin			PMFs		
		F	k_1	k_2	F	k_1	k_2	F	k_1	k_2
120	1	0.297^{h}	0.0707^{f}	0.0009^{g}	0.623^{e}	0.0945^{f}	0.0000^{g}	0.606^{f}	0.0968^{g}	0.0050^{f}
	1.5	0.448^{f}	0.0808^{e}	0.0009^{g}	0.702^{d}	0.1332^{e}	0.0000^{g}	0.698^{e}	0.1063^{f}	0.0043^{g}
	2	0.611^{d}	0.1031^{d}	0.0006^{g}	0.774^{bc}	0.2103^{c}	0.0000^{g}	0.740^{d}	0.1608^{c}	0.0011^{h}
140	1	0.339^{g}	0.0826^{e}	0.0065^{c}	0.642^{e}	0.0997^{f}	0.0096^{b}	0.692^{e}	0.1064^{f}	0.0085^{c}
	1.5	0.523^{e}	0.1067^{d}	0.0050^{e}	0.744^{c}	0.1648^{d}	0.0031^{e}	0.759^{d}	0.1170^{e}	0.0064^{d}
	2	0.748^{b}	0.1318^{c}	0.0041^{f}	0.784^{b}	0.2529^{b}	0.0017^{f}	0.838^{c}	0.1810^{b}	0.0052^{f}
160	1	0.652^{c}	0.1039^{d}	0.0093^{a}	0.704^{d}	0.0951^{f}	0.0243^{a}	0.759^{d}	0.1163^{e}	0.0201^{a}
	1.5	0.767^{b}	0.1535^{b}	0.0083^{b}	0.752^{bc}	0.1707^{d}	0.0074^{c}	0.916^{b}	0.1312^{d}	0.0111^{b}
	2	0.904^{a}	0.1701^{a}	0.0060^{d}	0.838^{a}	0.2795^{a}	0.0060^{d}	0.957^{a}	0.2043^{a}	0.0057^{e}

PMFs (polymethoxyflavones); sinensetin, nobiletin, and tangeretin, F; fast released fraction, k_1 and k_2: fast and slow desorption rate constants.

Data are expressed as the mean ± standard deviation of triplicate extractions.

The means in each column followed by the same letter are not significantly different by Duncan's multiple range test at $p < 0.05$.

2.4.3. Adjustment quality between the experimental data and each model

To verify the adjustment quality between the experimental data and each model, the correlation coefficient (R^2) and root mean squared error (RMSE) were calculated using Microsoft Excel 2010 Solver (Microsoft Corp., Redmond, WA, USA) and Eq. (3), respectively (Table 4).

$$\mathrm{RMSE} = \sqrt{\sum_{i=1}^{n} \frac{((\frac{C}{C_0})_{exp} - (\frac{C}{C_0})_{model})^2}{n}} \quad (3)$$

where C_0 is the initial solute content (mg/g) in the sample, C is the solute content (mg/g) extracted after time t (min), and n is the number of data.

The thermodynamic partitioning model showed relatively high R^2 ($\geq$ 0.946) and low RMSE ($\leq$ 0.08) values, indicating a good fit under some extraction conditions, such as during the initial stage. Meanwhile, the two-site kinetic desorption model showed the highest R^2 value ($\geq$ 0.988) and lowest RMSE value ($\leq$ 0.03) for the entire extraction period, suggesting that the SWE behaviors of citrus flavonoids were mainly controlled by intra-particle diffusion. The two-site kinetic model achieved better results than the thermodynamic partitioning model because it included additional parameters, such as k_2. Interestingly, the theoretical curves of the two-site kinetic model fit at all temperatures, even including the pyrolysis temperature (180 °C). Therefore, we conclude that the two-site kinetic model well described the decomposition mechanism, as well as the extraction mechanism, of citrus flavonoids when using SW: this study is the first to report this finding. Many of the kinetic curves reported for SWE also showed fast and slow extraction behaviors relating to molecules that were less and more strongly bonded, respectively, to the sample matrix (Ho et al., 2008; Barrera Vázquez et al., 2015; Duba et al., 2015).

Table 4. Coefficient of determination and root mean squared error obtained by regression analysis between the experimental and model data.

Temperature (°C)	Flow rate (mL/min)	Hesperidin				Narirutin				PMFs			
		K_D model		Two-site kinetic		K_D model		Two-site kinetic		K_D model		Two-site kinetic	
		R^2	RMSE ($\times 10^2$)	R^2	RMSE ($\times 10^2$)	R^2	RMSE ($\times 10^2$)	R^2	RMSE ($\times 10^2$)	R^2	RMSE ($\times 10^2$)	R^2	RMSE ($\times 10^2$)
120	1	0.979	3.09	0.991	1.03	0.988	3.94	0.999	0.34	0.985	3.82	0.996	1.80
	1.5	0.974	3.77	0.994	1.25	0.962	6.23	0.996	1.47	0.985	5.03	0.995	2.18
	2	0.991	2.80	0.997	0.90	0.977	5.53	0.997	1.25	0.990	4.78	0.998	1.86
140	1	0.996	4.50	0.995	1.19	0.994	2.96	0.999	0.77	0.989	3.56	0.995	2.16
	1.5	0.987	5.72	0.995	1.58	0.971	5.97	0.999	0.73	0.984	5.32	0.990	2.80
	2	0.994	3.14	0.998	0.85	0.981	5.18	0.997	2.24	0.991	3.89	0.997	1.74
160	1	0.998	3.69	0.999	0.67	0.998	1.68	0.999	0.67	0.999	1.54	0.994	3.39
	1.5	0.984	4.91	0.993	2.18	0.990	4.23	0.995	2.41	0.997	2.29	0.999	2.40
	2	0.989	3.46	0.988	3.46	0.985	4.40	0.993	2.90	0.996	2.22	0.998	1.28
180	1	0.946	7.57	0.999	0.56	0.970	6.68	0.999	0.48	0.979	5.34	0.999	2.62
	1.5	0.955	8.33	0.999	0.40	0.975	6.70	0.999	0.33	0.987	5.00	0.999	1.44
	2	0.955	7.97	0.994	1.78	0.955	7.81	0.998	0.85	0.965	7.01	0.999	0.73

PMFs, (polymethoxyflavones); sinensetin, nobiletin, and tangeretin, R^2: coefficient of determination, RMSE: root mean squared error.

2.5. Diffusion coefficient

To evaluate the mass transfer characteristics in SWE of citrus flavonoids, the effective diffusion coefficient (D_e, m^2/s) was calculated using the following equation (Asl and Khajenoori, 2013):

$$1 - \frac{C}{C_0} = \frac{6}{\pi^2} \exp(-\frac{D_e \pi^2 t}{r^2}) \quad (4)$$

where C and C_0 are the mass of solute (mg/g) extracted after time, t (min), and in the raw sample, respectively, and r is the radius (mm) of the particle, assumed to be spherical.

D_e was calculated from the gradient (= D_e π^2/r^2) of the linear portion of a plot of ln(1 − [C/C_0]) against t (R^2 > 0.95; Table 5 and Fig. 6). The D_e values of hesperidin and narirutin increased with temperature and flow rate. Especially, the D_e value of hesperidin at 120 °C and 1 mL/min was only 0.13 × 10^{-9} m^2/s, but increased about 9.8 times at 160 °C and 2 mL/min (1.28 × 10^{-9} m^2/s). The D_e values of PMFs also increased from 0.42 × 10^{-9} at 120 °C and 1 mL/min to 1.62 × 10^{-9} at 160 °C and 2 mL/min. The increases in the D_e values of all flavonoids were more affected by flow rate than by temperature. These increases in D_e values with temperature may be attributable to the increase in internal energy and mobility of the solute at higher temperatures (Ho et al., 2008). Their increases with flow rate may be due to the higher concentration gradient between the sample and the solvent, causing more rapid intra-particle diffusion (Al-Hamimi et al., 2016; Mottahedin et al., 2017). Islam et al. (2013) reported that the D_e values of phenanthrene, fluoranthene, and pyrene during SWE from Heukeumgi soil increased from 0.37 × 10^{-9}, 0.38 × 10^{-9}, and 0.30 × 10^{-9} cm^2/s to 1.45 × 10^{-9}, 1.35 × 10^{-9}, and 1.67 × 10^{-9} cm^2/s, respectively when the temperature increased from 200 °C to 250 °C. Kim and Mazza

(2007) also reported that D_e of phenolics from flax shives increased from 1.5 × 10^{-11} to 5.8 × 10^{-11} m^2/s as the flow rate increased from 0.5 to 2 mL/min at 180 °C.

Table 5. Diffusion coefficients of flavonoids at different extraction temperatures and flow rates.

Temperature (°C)	Flow rate (mL/min)	Diffusion coefficient (× $10^{-9}m^2/s$)		
		Hesperidin	Narirutin	PMFs
120	1	0.13 ± 0.01^{f}	0.36 ± 0.02^{g}	0.42 ± 0.02^{g}
	1.5	0.21 ± 0.01^{e}	0.49 ± 0.01^{ef}	0.51 ± 0.01^{f}
	2	0.25 ± 0.01^{e}	1.17 ± 0.10^{c}	0.78 ± 0.03^{d}
140	1	0.19 ± 0.01^{e}	0.44 ± 0.02^{f}	0.49 ± 0.02^{f}
	1.5	0.34 ± 0.02^{d}	0.69 ± 0.04^{d}	0.64 ± 0.03^{e}
	2	0.72 ± 0.02^{b}	1.33 ± 0.06^{b}	1.08 ± 0.06^{b}
160	1	0.43 ± 0.01^{c}	0.56 ± 0.02^{e}	0.52 ± 0.01^{f}
	1.5	0.77 ± 0.02^{b}	0.76 ± 0.01^{d}	0.88 ± 0.01^{c}
	2	1.28 ± 0.09^{a}	1.67 ± 0.08^{a}	1.62 ± 0.06^{a}

PMFs (polymethoxyflavones); sinensetin, nobiletin, and tangeretin.

Data are expressed as the mean ± standard deviation of triplicate extractions.

The means in each column followed by the same letter ($^{a-f}$) are not significantly different by Duncan's multiple range test at $p < 0.05$.

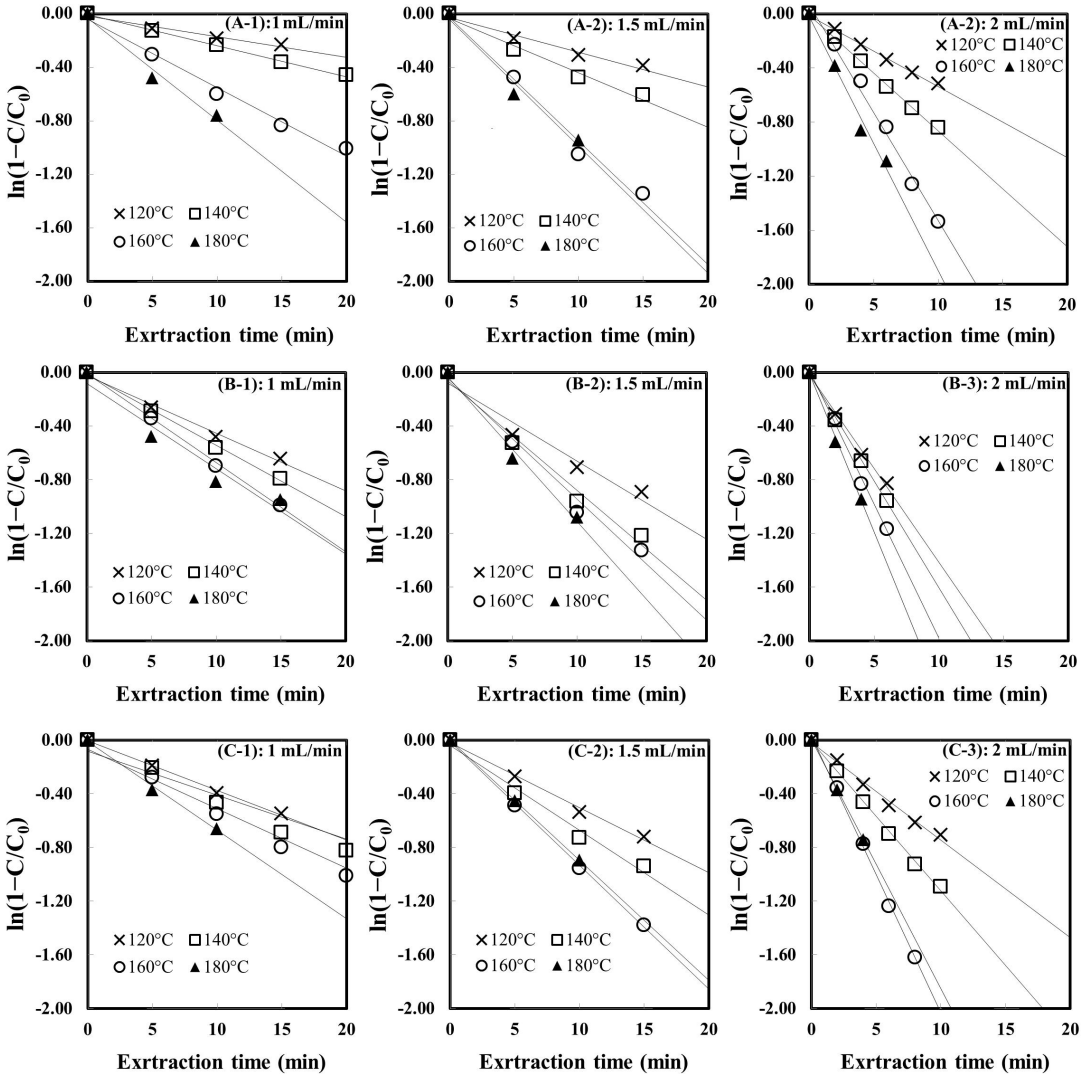

Fig. 6. Application of diffusion coefficient of flavonoids extraction using SWE at different extraction temperatures and flow rates. (A) hesperidin, (B) narirutin, (C) PMFs (sinensetin + nobiletin + tangeretin).

2.6. Activation energy

Activation energy (E_a) is an energy barrier that must be overcome for extraction to occur. If the *Ea* required to extract a certain component is high, then the extraction rate is reduced. The E_a (kJ/mol) for diffusion at different flow rates were calculated using the Arrhenius equation (Islam et al., 2013):

$$D_e = D_0 \exp(-\frac{E_a}{RT}) \quad (5)$$

where D_e and D_o are the effective and initial diffusion coefficients (m^2/s), respectively, T is the absolute temperature (K), and R is the molar gas constant (J·K/mol).

The E_a values were calculated at different flow rates based on the values of D_e for 120, 140, and 160 °C (Table 6 and Fig. 7). The diffusivity obtained at 180 °C was not used for calculating E_a due to the degradation of flavonoids at that temperature. The values of E_a for hesperidin at all flow rates (37.2－43.8 kJ/mol) were higher than those of other flavonoids (8.2－36.8 kJ/mol), probably due to its low solubility in water (Céliz et al., 2014). The E_a values of hesperidin and narirutin decreased slightly, from 42.3 to 37.2 kJ/mol and from 15.5 to 12.0 kJ/mol, respectively, when the flow rate increased from 1 to 2 mL/min. This is probably because the higher flow rate disrupted the solute‐solute and solute‐matrix interactions (Richter et al., 1996; Ho et al., 2008). Cacace and Mazza (2003) reported high E_a values of 70‐97 kJ/mol for the diffusion of anthocyanins and all phenolics from blackcurrants.

By contrast, the E_a value of PMFs increased from 7.1 to 25.8 kJ/mol when the flow rate increased from 1 to 2 mL/min. Plaza and Turner (2015) reported that the polarity (dielectric constant) of water decreases, but the dipole moment of water

molecules does not change under subcritical conditions. Therefore, the diffusion of PMFs may be inhibited by the hydrophobic interactions between the sample matrices and PMF molecules, because PMFs are highly nonpolar compounds due to the large number of methoxyl groups in their molecular structures (Lai et al., 2015). Further study is needed on the correlation between the molecular structures of citrus flavonoids and the E_a values for their diffusion at different flow rates.

Table 6. Activation energies for diffusion of flavonoids during subcritical water extraction.

Flow rate (mL/min)	Activation energy (kJ/mol)		
	Hesperidin	Narirutin	PMFs
1	42.3 ± 2.3[a]	15.5 ± 1.5[a]	7.1 ± 0.6[c]
1.5	43.8 ± 1.8[a]	15.6 ± 1.0[a]	19.2 ± 1.2[b]
2	37.2 ± 2.2[b]	12.0 ± 0.8[b]	25.8 ± 0.1[a]

PMFs (polymethoxyflavones); sinensetin, nobiletin, and tangeretin.

Data are expressed as the mean ± standard deviation of triplicate extractions.

The means in each column followed by the same letter ([a-c]) are not significantly different by Duncan's multiple range test at $p < 0.05$.

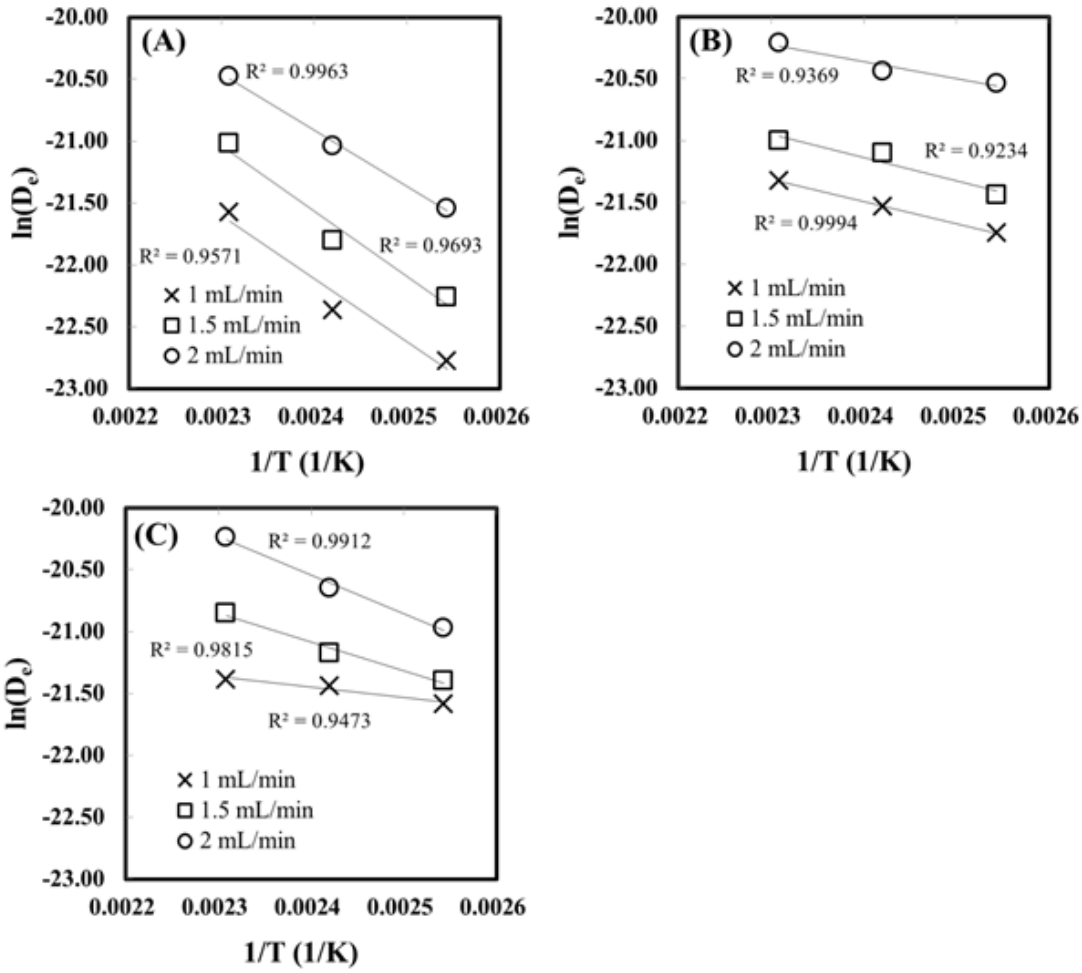

Fig. 7. Arrhenius-type relationship between diffusion coefficient and temperature for flavonoids extraction using SWE at different extraction flow rates. (A), hesperidin; (B), narirutin; (C), PMFs (sinensetin + nobiletin + tangeretin).

2.7. Comparison with organic solvent extractions

The flavonoid yields in SWE were compared with those of conventional organic solvent extractions (Table 7). The hesperidin yield by SWE was more than 1.4, 2.4, and 5.8 times higher, the narirutin yield was more than 1.1, 1.2, and 5.6 times higher, and the PMFs yield was more than 1.1, 1.4, and 1.6 times higher than those obtained by conventional extractions using methanol, ethanol, and acetone, respectively. Organic solvents such as methanol, ethanol, and acetone are often used for extraction of flavonoids, but their use is limited by toxic residue, complete removal process, etc (Lachos-Perez et al., 2018). Thus, SW could be an efficient alternative to organic solvents for extracting flavonoids in terms of extraction efficiency and environmental friendly process (Mortazavi et al., 2010).

Table 7. Comparison of solvents for flavonoid extraction from *Citrus unshiu* peel.

	Flavonoid content (μg/g dry sample)			
	Subcritical water (160 °C)	Methanol (65 °C)	Ethanol (78 °C)	Acetone (56 °C)
Hesperidin	42,538 ± 2,133^{a}	30,891 ± 1,179^{b}	17,360 ± 696^{c}	7,225 ± 557^{d}
Narirutin	8,007 ± 198^{a}	6,993 ± 328^{b}	3,612 ± 190^{c}	1,426 ± 123^{d}
PMFs	161 ± 2^{a}	139 ± 3^{b}	112 ± 4^{c}	97 ± 1^{d}
Total	50,708 ± 2,317^{a}	38,024 ± 1,497^{b}	21,084 ± 871^{c}	8,749 ± 681^{d}

Extraction time: 15 min, solvent to feed ratio: 30 mL/g.

Data are expressed as the mean ± standard deviation of triplicate extractions.

The means in each row followed by the different letter ($^{a-d}$) are significantly different by Duncan's multiple range test at $p < 0.05$.

3. Conclusion

Hesperidin, narirutin, and PMFs (sinensetin, nobiletin, and tangeretin) were extracted from *Citrus unshiu* peel using a semi-continuous SWE system at different temperatures and flow rates. The extraction mechanism was evaluated by adjusting the parameters of thermodynamic partitioning and two-site kinetic desorption models to the experimental data. The extraction rates of citrus flavonoids showed direct proportionality to temperature and flow rate with SW. The SWE rate curve indicated both fast and slow extraction behaviors, associated with molecules that were less and more strongly coupled, respectively, to the sample matrix. The two-site kinetic desorption model best described the decomposition mechanism, as well as the extraction mechanism, of citrus flavonoids with SW. D_e of citrus flavonoids was more affected by the flow rate than the temperature. E_a for diffusion of flavonoids differed depending on the polarity of the citrus flavonoids. SWE is a promising technology for extracting flavonoids from *Citrus unshiu* peel with high yields within a short time, using an environmentally friendly solvent (water).

Part. Ⅱ

Subcritical Water Extraction of Flavonoids from *Citrus unshiu* peel: Their Biological Activity

1. Materials and Methods

1.1. Sample preparation

The same as in Part 1.

1.2. Chemicals

Hesperidin, hesperetin, narirutin, naringenin, DPPH, 2,4,6-tris(2-pyridyl)-s-triazine (TPTZ), ferrous sulfate heptahydrate, fluorescein sodium salt, N-hippuryl-his-leu hydrate (HHL), lung acetone powder from rabbit, xanthine oxidase from bovine milk, allopurinol, ρ-nitrophenyl-β-D-glucopyranoside (ρ-NPG), acarbose, α-glucosidase from Saccharomyces cerevisiae, ρ-nitrophenyl butyrate (ρ-NPB), lipase from porcine pancreas, orlistat, and 3-(N-Morpholino)propane sulfonic acid (MOPS) were purchased from Sigma Chemical Co. (St. Louis, MO). 2,2'-Azobis (2-methylpropionamidine) dihydrochloride (AAPH) was purchased from Acros organics (Geel, Belgium) and captopril was purchased from Tokyo Chemical Industry Co., Ltd. (Kita-ku, Tokyo, Japan). Sinensetin, nobiletin, and tangeretin were purchased from Avention (Yeonsu-gu, Incheon, Republic of Korea). Hesperetin-7-O-glucoside and prunin were purchased from Extrasynthese (Genay, France). Acetic acid was purchased from Junsei Chemical Co., Ltd (Chuo-ku, Tokyo, Japan) and HPLC grade acetonitrile and methyl alcohol were purchased from Daejung Chemicals & Metals Co., Ltd (Shiheung, Gyeonggi, Republic of Korea).

1.3. Subcritical water extraction

The same as in Part 1 except the followings. Extracts were collected for 15 min. Individual flavonoid concentrations were quantified using HPLC, and the functional properties were analyzed for each extract. The percentage soluble content (%) of each extract (as a solid) was calculated relative to the total solid content after drying at 105 °C.

1.4. Acid and base hydrolysis

Acid and base hydrolysis of the peel powders was performed as described previously (Chen et al., 2015) with some modifications. In the case of acid hydrolysis, samples consisting of 1 g of peel powder were hydrolyzed in 20 mL of 2 M HCl for 60 min at 85 °C with shaking (120 rpm). The hydrolysis solution was allowed to cool to room temperature, adjusted to pH 2.0 using 12 M NaOH, and then centrifuged at 10,000 rpm for 10 min. The supernatant was recovered, and the residue was washed two more times by adding 20 mL of neat methanol and vortexing for 1 min. The hydrolysate was then concentrated and filtered (0.45 μm) before the HPLC analysis.

For base hydrolysis, samples consisting of 1 g of peel powder were hydrolyzed in 20 mL of 2 M NaOH (containing 10 mM EDTA and 1% ascorbic acid) for 4 h at 25 °C with shaking (120 rpm). The hydrolysis solution was adjusted to pH 2.0 using 12 M HCl and then centrifuged at 10,000 rpm for 10 min. The supernatant was recovered and the residue was washed two more times with 20 mL of neat methanol with vortexing. The hydrolysate was then concentrated and filtered (0.45 μ m) before the HPLC analysis.

1.5. HPLC analysis

Hesperidin and its hydrothermal hydrolysis products (HHP) (hesperetin-7-O-glucoside and hesperetin), narirutin and its HHP (prunin and naringenin), and PMFs (sinensetin, nobiletin, and tangeretin) in the SW extracts were quantified using an HPLC system. The rest of them are the same as in Part 1.

1.6. Response surface design

The SWE of citrus flavonoids was optimized using RSM. A central composite design was selected to optimize the relationships between the response variables and two independent variables-temperature (X_1: 145－175 °C) and flow rate (X_2: 0.75－2.25 mL/min). The quadratic polynomial was used to predict the optimal extraction conditions based on experimental data with the following equation:

$$Y = \beta_0 + \beta_1 X_1 + \beta_2 X_2 + \beta_{11} X_1^2 + \beta_{22} X_2^2 + \beta_{12} X_1 X_2 \quad (6)$$

where X_1 and X_2 are levels of independent variables, Y is the response variable, and β_0, β_1, β_2, β_{11}, β_{22}, and β_{12} are coefficients. The fit of each model was evaluated via analysis of variance (ANOVA) using Design Expert® software (Stat-Ease Inc., Minneapolis, MN, USA).

1.7. Antioxidant activity measurement

The antioxidant activities－DPPH radical scavenging activity, FRAP, and ORAC－of the SW extracts and individual flavonoids were measured. DPPH radical scavenging activity was measured as described previously (Ye et al., 2019) with some modifications. Briefly, a 0.5-mL sample was mixed with 2.0 mL DPPH solution (0.2 mM), and the mixture was allowed to react for 30 min in the dark. The absorbance was then measured at 517 nm. DPPH radical scavenging activity was expressed as mg ascorbic acid equivalents (AAE)/g dry sample.

FRAP was measured as described previously (Ye et al., 2019) with some modifications. Briefly, the FRAP reagent was prepared by mixing 300 mM acetate buffer, 20 mM $FeCl_3 \cdot 6H_2O$, and 10 mM TPTZ at a ratio of 1:1:10 (v/v). A 0.2-mL sample was mixed with 3 mL of FRAP reagent and 0.3 mL of distilled water and allowed to react for 30 min at 37 °C. The absorbance was then measured at 595 nm. FRAP was expressed as mmol ferrous sulfate equivalents (FSE)/100 g dry sample.

ORAC was measured as described previously (Ye et al., 2019) with some modifications. Briefly, a 0.025-mL sample was mixed with 0.15 mL of fluorescein sodium salt solution (78 nM) and allowed to react for 15 min at 37 °C. Then, 0.025 mL of AAPH (250 mM) was added to the solution, and the fluorescence was measured every 3 min for 120 min (excitation, 485 nm; emission, 535 nm). The area under the curve was calculated for each sample and compared to that of a Trolox standard. ORAC was expressed as mg Trolox equivalents (TE)/g dry sample.

1.8. Biological activity measurement

Enzyme inhibitory activities (against XO, ACE, α-glucosidase, and PL) in the SW extracts and individual flavonoids were measured. A stock solution of each flavonoid standard was prepared by dissolving the standard in dimethyl sulfoxide (DMSO), and the working solution was prepared by dissolving standards in suitable buffer solutions for each experiment. The final DMSO concentration was ≤ 5% (v/v), which did not affect enzyme activities.

XO inhibitory activity was measured as described previously (Yoon and Jang, 2018) with some modifications. Briefly, a 0.1-mL sample was mixed with 0.3 mL of phosphate buffer (50 mM, pH 7.5) and 0.1 mL of 0.5 U/mL XO solution (in 50 mM phosphate buffer, pH 7.5). The reaction mixture was incubated for 15 min at 25 °C. Then, 0.2 mL of 2 mM xanthine solution was added, and the mixture was incubated for 30 min at 25 °C. The enzyme reaction was stopped with 0.3 mL of 1 M HCl. The reaction mixture was diluted with distilled water, and the absorbance was measured at 290 nm. Allopurinol was used as a positive control.

ACE inhibitory activity was measured as described previously (Hussain et al., 2018) with some modifications. Briefly, a 0.05-mL sample was mixed with 0.1 mL HHL solution (12.5 mM) and incubated for 5 min at 37 °C. Then, 0.15 mL of ACE solution (in 50 mM phosphate buffer, pH 7.3) was added, and the mixture was re-incubated for 60 min at 37 °C. The enzyme reaction was stopped with 0.25 mL of 1 M HCl, and the hippuric acid in the reaction mixture was extracted by adding 1.5 mL of ethyl acetate. After centrifugation at 4,000 rpm for 5 min, 1.0 mL of the supernatant was transferred to a clean tube and evaporated. Then, 1 mL of distilled water was added to dissolve the dry residue, and the absorbance was measured at 228 nm. Captopril was used as a positive control.

The α-glucosidase inhibitory activity was measured as described previously (Proenca et al., 2017) with some modifications. Briefly, a 0.05-mL sample was mixed with 0.1 mL of phosphate buffer (100 mM, pH 6.8) and 0.05 mL of α-glucosidase

solution (1 U/mL, in 100 mM phosphate buffer, pH 6.8). The enzyme mixture was incubated for 15 min at 37 °C. Then, 0.1 mL of ρ-NPG (3 mM) was added, and the mixture was re-incubated for 10 min at 37 °C. The enzyme reaction was stopped with 0.45 mL of Na_2CO_3 (0.1M), and the absorbance was measured at 405 nm. Acarbose was used as a positive control.

PL inhibitory activity was measured as described previously (Kim et al., 2014) with some modifications. Briefly, a 5 mg/mL enzyme solution was prepared by dissolving porcine PL in MOPS buffer (10 mM MOPS and 1 mM EDTA, pH 6.8). A 0.025-mL sample was mixed with 0.9 mL Tris-HCl buffer (100 mM Tris-HCl and 5 mM $CaCl_2$, pH 7.0) and 0.025 mL of enzyme solution (5 U/mL). The enzyme mixture was incubated for 15 min at 37 °C. Then, 0.05 mL of ρ-NPB (10 mM) was added, and the mixture and re-incubated at 37 °C for 30 min. The absorbance was measured at 405 nm. Orlistat was used as a positive control.

1.9. Statistical analysis

The same as in Part 1 except the followings. Pearson correlation coefficients (*r*) representing the relationships between flavonoid contents and functional properties were also calculated using SPSS software (SPSS Inc., Chicago, IL, USA).

2. Results and Discussion

2.1. Optimization of SWE process

Table 8 presents the yields of hesperidin and its HHP (hesperetin-7-O-glucoside and hesperetin), narirutin and its HHP (prunin and naringenin), and PMFs (sinensetin, nobiletin, and tangeretin) in the SW extracts of citrus peel at different temperatures and flow rates. Table 9 presents the results of ANOVA and regression analysis for the five flavonoids. All regression models produced high R^2 values (> 0.966), low p-values (< 0.05), and non-significant lack-of-fit p-values (> 0.05), indicating that the regression models provided good fits. Moreover, smaller differences (< 0.2) between adjusted and predicted R^2 values, low %C.V. values ($\leq$ 5%), and high adequate precision (> 16) also indicated that the regression models provided good fits (Ravber et al., 2015).

The optimal extraction conditions for maximizing the yields of the five flavonoids were estimated using the following second-order polynomial equations:

$$Y(\text{hesperidin}) = 37{,}098 + 2{,}470X_1 + 6{,}609X_2 - 2{,}411X_1^2 - 1{,}016X_2^2 - 204X_1X_2 \quad (7)$$

$$Y(\text{narirutin}) = 6{,}821 + 4.4X_1 + 1{,}277X_2 - 68.5X_1^2 + 3.8X_2^2 - 50.6X_1X_2 \quad (8)$$

$$Y(\text{sinensetin}) = 16.19 - 0.62X_1 + 2.01X_2 - 0.49X_1^2 - 0.69X_2^2 - 0.55X_1X_2 \quad (9)$$

$$Y(\text{nobiletin}) = 83.37 + 2.51X_1 + 8.71X_2 - 1.44X_1^2 - 2.55X_2^2 - 0.59X_1X_2 \quad (10)$$

$$Y(\text{tangeretin}) = 41.52 + 1.76X_1 + 8.01X_2 - 1.36X_1^2 + 0.02X_2^2 - 1.10X_1X_2 \quad (11)$$

where Y is the yield, X_1 is temperature, and X_2 is flow rate.

Based on the models, the optimal extraction temperatures of hesperidin, narirutin, sinensetin, nobiletin, and tangeretin were 164.4 °C, 154.6 °C, 145.3 °C, 165.6 °C, and 160.5 °C, respectively, and the optimal flow rate was 2.25 mL/min (Table 10).

The predicted yields of hesperidin, narirutin, sinensetin, nobiletin, and tangeretin at the optimal extraction conditions were 45,211, 8,765, 18.7, 91.2, and 53.6 μg/g dry sample, respectively, which were 90.4%, 94.4%, 98.9%, 87.8%, and 96.6%, respectively, of the corresponding raw material contents. The optimal SWE conditions for simultaneous extraction of the five flavonoids were a temperature of 158.5 °C and a flow rate of 2.25 mL/min, which resulted in maximum yields of 88.7%, 94.3%, 94.2%, 87.1%, and 96.4% for hesperidin, narirutin, sinensetin, nobiletin, and tangeretin, respectively. The relationships between the responses (flavonoid yields) and experimental variables (extraction temperature and flow rate) are presented in the response surface plots in Fig. 8.

Table 8. Central composite design and corresponding flavonoid and total soluble solid yields in subcritical water extracts from *Citrus unshiu* peel.

No	X_1	X_2	Hesperidin and its hydrolysis products (μg/g dry sample)			Narirutin and its hydrolysis products (μg/g dry sample)			Polymethoxyflavones (μg/g dry sample)			Total flavonoids (μg/g dry sample)	Total soluble solids (%)	Total flavonoid concentration in the extract (mg/g dry extract)
			Hesperidin	Hesperetin-7-O-glucoside	Hesperetin	Narirutin	Prunin	Naringenin	Sinensetin	Nobiletin	Tangeretin			
1	150	1	24,700.4	N.D.	N.D.	5,442.7	N.D.	N.D.	13.7	68.8	29.0	30,253.5	45.2 ± 0.3^{d}	66.6
2	150	2	37,995.1	N.D.	N.D.	8,040.6	N.D.	N.D.	18.4	85.4	45.5	46,184.3	56.0 ± 1.7^{bc}	82.4
3	170	1	30,498.0	1,640.8	1,591.0	5,631.8	237.8	222.3	13.2	76.4	37.4	39,947.9	58.2 ± 2.4^{ab}	68.5
4	170	2	42,975.4	756.8	937.1	8,027.2	200.4	145.7	15.7	90.6	49.6	53,197.9	57.9 ± 1.5^{ab}	91.8
5	145	1.5	27,935.1	N.D.	N.D.	6,687.7	N.D.	N.D.	15.6	76.5	37.5	34,751.6	38.5 ± 1.1^{e}	90.1
6	175	1.5	34,749.8	2,048.0	1,802.7	6,595.3	326.0	268.1	14.2	82.2	39.1	45,924.3	58.1 ± 0.7^{ab}	79.0
7	160	0.75	24,345.7	698.2	433.6	4,848.1	162.5	102.3	11.1	62.4	28.2	30,691.3	45.3 ± 1.2^{d}	67.6
8	160	2.25	44,617.3	370.6	642.5	8,760.0	N.D.	135.2	17.7	91.2	54.5	54,688.7	60.6 ± 2.2^{a}	90.1
9	160	1.5	36,858.1	757.8	870.2	6,856.2	141.4	126.1	15.9	82.5	41.6	45,749.5	55.1 ± 0.6^{c}	82.9
10	160	1.5	36,786.7	701.2	856.7	6,832.4	135.9	127.7	16.6	83.9	40.8	45,580.8	---	75.1
11	160	1.5	37,486.7	739.4	884.1	6,762.1	142.1	135.1	15.9	83.2	42.1	46,289.9	---	76.3

X_1: temperature (°C), X_2: flow rate (mL/min), N.D.: not detected.

The same superscript letters in each column ($^{a-d}$) indicate no significant differences ($p < 0.05$).

Table 9. Analysis of variance for regression models.

Source	Hesperidin		Narirutin		Sinensetin		Nobiletin		Tangeretin	
	F-value	*p*-value	*F*-value	*p*-value	*F*-value	*p*-value	*F*-value	*p*-value	*F*-value	*p*-value
Model	245.79	< 0.0001	476.95	< 0.0001	33.03	0.0008	41.40	0.0005	28.62	0.0011
X_1	137.85	< 0.0001	0.03	0.8708	12.67	0.0162	14.87	0.0119	6.36	0.0531
X_2	986.57	< 0.0001	2,376.63	< 0.0001	133.22	< 0.0001	178.96	< 0.0001	132.15	< 0.0001
X_1^2	103.29	0.0002	5.37	0.0682	6.31	0.0537	3.87	0.1064	2.98	0.1447
X_2^2	18.35	0.0078	0.02	0.9010	12.59	0.0164	12.05	0.0178	0.00	0.9814
X_1X_2	0.44	0.5348	1.76	0.2425	4.74	0.0814	0.39	0.5600	1.17	0.3284
Lack of fit	3.56	0.2270	3.40	0.2355	1.92	0.3602	11.20	0.0831	13.71	0.0688
R^2	0.9959		0.9979		0.9706		0.9764		0.9662	
pred R^2	0.9742		0.9867		0.8267		0.8371		0.7641	
adj R^2	0.9919		0.9958		0.9412		0.9528		0.9325	
C.V%	1.78		1.13		3.33		2.36		5.02	
Adeq precision	44.8		67.9		17.5		18.64		16.1	

X_1: temperature (°C), X_2: flow rate (mL/min), pred R^2: predicted R^2, adj R^2: adjusted R^2, C.V: coefficient of variance, Adeq precision: adequate precision.

Table 10. Subcritical water extraction parameters for maximizing flavonoid yields from *Citrus unshiu* peel.

	Temperature (°C)	Flow rate (mL/min)	Predicted yield		Desirability
			μg/g dry sample	%	
Hesperidin (H)	164.4	2.25	45,211.0	90.4	1
Narirutin (N)	154.6	2.25	8,765.2	94.4	1
Sinensetin (S)	145.3	2.25	18.7	98.9	1
Nobiletin (NO)	165.6	2.25	91.2	87.8	1
Tangeretin (T)	160.5	2.25	53.6	96.6	1
H+N	159.5	2.25	44,622.4/8,749.7	89.1/ 94.2	1
S+NO+T	153.5	2.25	18.4/89.0/52.9	97.3/85.7 /95.3	0.8603
H+N+S+ NO+T	158.5	2.25	44,366.4/8,755.4 /17.8/90.4/53.5	88.7/94.3 /94.2/87.1 /96.4	0.6389

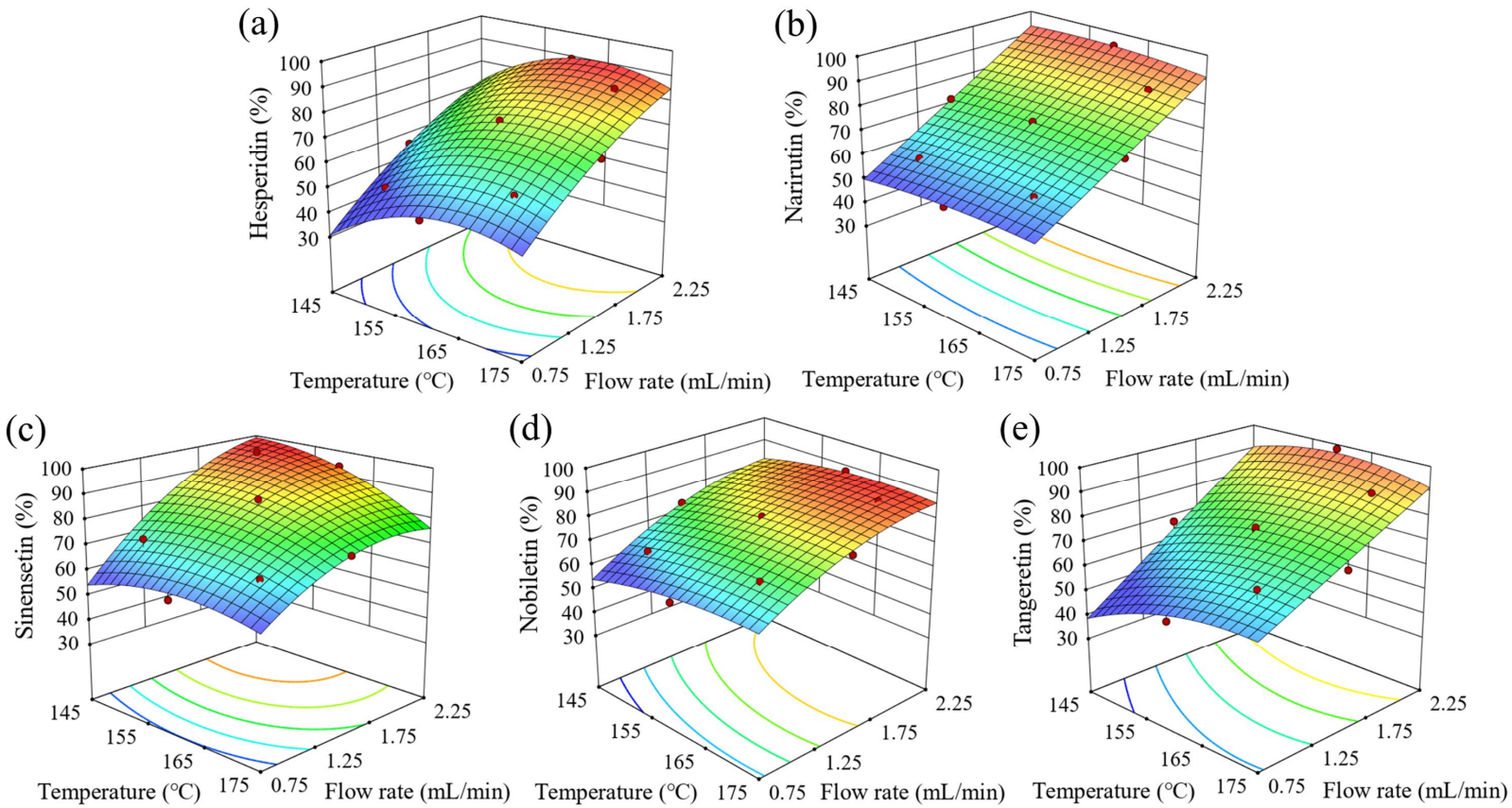

Fig. 8. Response surface plots indicating the effects of extraction temperature and flow rate on flavonoid yields: (a) hesperidin, (b) narirutin, (c) sinensetin, (d) nobiletin, and (e) tangeretin.

2.2. Effects of extraction parameters on individual flavonoid yields

Table 8 and Fig. 8 present individual flavonoid yields in the SW extracts at different temperatures and flow rates. The hesperidin yield increased with increasing extraction temperature from 145 °C to 165 °C. This was because the dielectric constant decreases as the temperature increases, which reduces the polarity of water. The dielectric constant of water at 20 °C is 80.2, but it decreases to 44.9 and 40.9 as the temperature increases to 145 °C and 165 °C, respectively (Brunner, 2013). Céliz et al. (2015) reported that the solubility of hesperidin increased by more than fivefold when the water temperature increased from 110 °C to 160 °C. Lachos-Perez et al. (2018) also reported that the hesperidin yield from defatted orange peel increased by 1.8－4.1-fold when the extraction temperature increased from 110 °C to 150 °C at different flow rates. However, the hesperidin yield decreased at temperatures higher than 165 °C because hesperidin was hydrolyzed to its monoglucoside (hesperetin-7-O-glucoside) or aglycone (hesperetin) (Ruen-ngam et al., 2012).

By contrast, the impact of temperature on the narirutin yield was not greater than that on the hesperidin yield due to the higher solubility of narirutin (compared to hesperidin) in water (Gil-Izquierdo et al., 2002). This was consistent with the low optimal extraction temperature (154.6 °C) of narirutin compared with that of hesperidin (164.4 °C) (Table 10). Park et al. (2012) reported that narirutin is water-soluble, whereas hesperidin is hardly soluble in water. The HHP of narirutin, such as prunin and naringenin, were also detected at temperatures higher than 160 °C, and their yields increased at higher temperatures and lower flow rates.

For PMFs, the nobiletin yield increased with increasing temperature from 145 °C to 165 °C and decreased slightly at temperatures above 165 °C at a flow rate of 2.25 mL/min (Fig. 8). The tangeretin yield also increased with increasing temperature from 145 °C to 160 °C at a flow rate of 2.25 mL/min. However, the sinensetin yield was highest at 145 °C due to its thermal instability (Zhang et al., 2019). The

optimal extraction temperature of sinensetin was low (145.3 °C), whereas those of nobiletin (165.6 °C) and tangeretin (160.5 °C) were high. Zhang et al. (2019) reported that the degradation ratio of sinensetin as represented by demethylation during hot-air drying was higher than those of nobiletin and tangeretin.

Table 8 and Fig. 8 also show the effects of water flow rates on flavonoid yields. The yields of individual flavonoids increased significantly with an increasing flow rate from 0.75 to 2.25 mL/min under subcritical conditions. This was because higher flow rates increased the extraction yield by increasing the concentration gradient, superficial velocity, and mass transfer rate between the extraction solvent and the sample matrix during SWE (Mottahedin et al., 2017; Kim and Lim, 2019). In particular, the extraction yield of narirutin was greatly affected by the flow rate because narirutin is more soluble in water compared to the other flavonoids. On the other hand, the hesperidin yield was influenced by the flow rate as well as temperature because it is less soluble in water compared to narirutin (Park et al., 2012). The PMF yields were also significantly affected by flow rate because they are less soluble in water.

The extraction yield of total soluble solids increased with increasing temperature and flow rate as well (Table 8). The sum of individual flavonoid contents in the raw material was 59.49 mg/g dry sample (Table 8), but that in the SW extract at 160 °C and 2.25 mL/min increased to 90.1 mg/g dry extract, corresponding to 9.0% of the extract.

2.3. Comparison of flavonoid profiles between SW extract and acid and base hydrolysis

The flavonoid composition in the SW extract at 175 °C and 1.5 mL/min was compared with those in the acid and base hydrolysates of citrus peel (Table 11). The yields of hesperidin and narirutin in the SW extract were 2.15－2.87-fold and 4.07－5.31-fold higher than those in the acid and base hydrolysates, respectively. Some of the hesperidin and narirutin were converted to their HHP in the SW extract, indicating that citrus flavonoid diglucosides can be hydrolyzed into highly functional low-molecular-weight compounds when they are treated with SW instead of an acid or base.

In the case of the acid hydrolysate, monoglucosides (hesperetin-7-O-glucoside and prunin) and aglycones (hesperetin and naringenin) were produced via the acid hydrolysis of glycosidic bonds between aglycone and sugar (Peng et al., 2018). However, the yields were very low, indicating that the generated aglycones had been decomposed into smaller molecules. In the case of the base hydrolysate, HHP such as monoglucosides and aglycones were not detected at all. This was due to the hydrolysis of esters and ether bonds, but not glycosidic bonds, via base hydrolysis (Peng et al., 2018). In the present study, several unknown peaks were detected in the base hydrolysate (Fig. 9), which indicate that flavanones were converted to chalcone derivatives under basic conditions (Andujar et al., 2003).

Table 11. Comparison of flavonoid profiles between SW extract and acid and base hydrolysis of *Citrus unshiu* peel.

	Flavonoid content (μg/g dry sample)		
	Subcritical water extract*	Acid hydrolysate	Base hydrolysate
Hesperidin	34,749.8	12,081.2 ± 1,188.3	16,124.1 ± 491.9
Hesperetin-7-O-glucoside	2,048.0	2,462.4 ± 96.0	N.D.
Hesperetin	1,802.7	2,204.0 ± 39.9	N.D.
Narirutin	6,595.3	1,240.7 ± 54.2	1,620.8 ± 8.3
Prunin	326.0	703.9 ± 23.6	N.D.
Naringenin	268.1	863.0 ± 34.5	N.D.
Sinensetin	14.2	18.3 ± 0.6	15.4 ± 0.3
Nobiletin	82.2	91.1 ± 0.7	74.3 ± 1.7
Tangeretin	39.1	57.6 ± 2.5	41.8 ± 1.1
Total	45,924.3	19,722.2 ± 1,236.3	17,876.4 ± 483.9

*Subcritical water extracts were processed at 175 ℃ and 1.5 mL/min; N.D., not detected.

Data are expressed as the mean ± standard deviation of triplicate experiments.

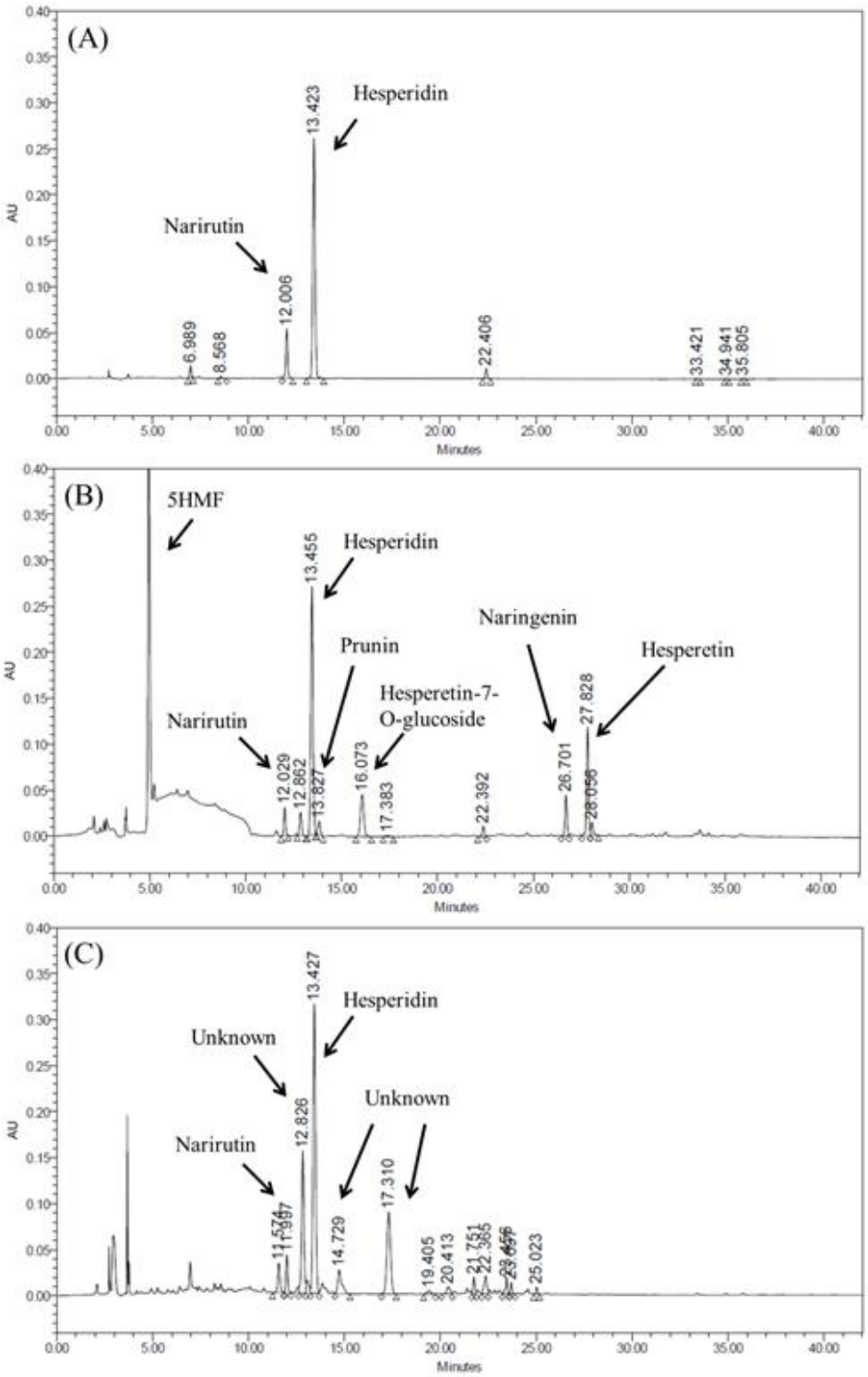

Fig. 9. High-performance liquid chromatography chromatograms of the (a) methanol extract, (b) acid hydrolysate, and (c) base hydrolysate of *Citrus unshiu* peel.

2.4. Biological activities of SW extracts

Table 12 presents the antioxidant activities (DPPH radical scavenging activity, FRAP, and ORAC) and enzyme inhibitory activities (against XO, ACE, α-glucosidase, and PL) in the SW extracts from *Citrus unshiu* peel processed at different temperatures and flow rates. DPPH radical scavenging activity in the SW extracts increased with increasing temperature and flow rate. The highest DPPH radical scavenging activity was obtained at 160 °C and 2.25 mL/min as well as 175 °C and 1.5 mL/min. FRAP and ORAC also exhibited similar trends as DPPH radical scavenging activity. Lachos-Perez et al. (2018) reported that the antioxidant capacities (DPPH radical scavenging activity, FRAP, and ORAC) of the SW extracts from defatted orange peel increased with increasing temperature (110－150 °C). Kanmaz and Saral (2018) reported that the SW extracts from mandarin peel exhibited high antioxidant activities (FRAP and cupric-reducing antioxidant capacity) at higher extraction temperatures and longer extraction times.

The enzyme inhibitory activities, such as those against XO, ACE, α-glucosidase, and PL, were also measured (Table 12). These activities are related to anti-gout, anti-hypertension, anti-diabetes, and weight-control effects, respectively (Kim et al., 2014; Proenca et al., 2017; Hussain et al., 2018; Yoon and Jang, 2018). The enzyme inhibitory activities in the SW extracts against XO, ACE, and α-glucosidase increased with increasing temperature and flow rate, and the highest activity was obtained at 175 °C and 1.5 mL/min. Nile et al. (2019) reported that XO and α-glucosidase inhibitory activities in Withania somnifera L extracts processed using SW increased with increasing temperature from 100 °C to 160 °C. In particular, the PL inhibitory activities in all SW extracts were higher compared to other enzyme inhibitory activities probably due to the high content of citrus flavonoids (Gironées-Vilaplana et al., 2014).

Table 12. Biological activities of subcritical water extracts from *Citrus unshiu* peel.

X_1	X_2	Antioxidant activity			Enzyme-inhibitory activity			
		DPPH radical scavenging activity (mg AAE/g dry sample)	FRAP (mmol FSE /100 g dry sample)	ORAC (mg TE/g dry sample)	Xanthine oxidase (%)	ACE (%)	α-Glucosidase (%)	Pancreatic lipase (%)
145	1.5	8.3 ± 0.1^{f}	24.7 ± 1.1^{f}	169.5 ± 5.2^{d}	11.6 ± 1.3^{f}	12.8 ± 1.5^{f}	12.8 ± 1.1^{f}	52.0 ± 1.9^{g}
150	1	8.2 ± 0.3^{f}	24.9 ± 0.9^{f}	122.8 ± 5.8^{e}	16.6 ± 1.4^{e}	14.2 ± 0.6^{ef}	16.5 ± 0.8^{e}	59.8 ± 1.9^{ef}
150	2	14.8 ± 0.5^{c}	28.9 ± 0.7^{e}	338.8 ± 16.6^{b}	20.8 ± 1.8^{d}	22.5 ± 1.3^{d}	21.4 ± 1.4^{d}	66.8 ± 2.0^{d}
160	0.75	9.5 ± 0.6^{e}	25.5 ± 0.9^{f}	281.3 ± 17.5^{c}	15.3 ± 1.0^{e}	16.2 ± 0.7^{e}	20.7 ± 1.2^{d}	58.0 ± 1.6^{f}
160	1.5	13.3 ± 0.7^{d}	45.3 ± 1.3^{c}	316.2 ± 26.3^{bc}	21.4 ± 0.8^{d}	21.6 ± 0.5^{d}	23.1 ± 1.1^{d}	64.1 ± 2.7^{de}
160	2.25	18.6 ± 0.3^{a}	48.8 ± 1.3^{b}	397.4 ± 21.8^{a}	30.9 ± 1.7^{c}	35.6 ± 1.5^{b}	41.0 ± 1.7^{bc}	73.3 ± 1.8^{c}
170	1	14.0 ± 0.0^{cd}	39.3 ± 1.1^{d}	327.6 ± 5.0^{b}	32.3 ± 1.8^{c}	32.6 ± 1.7^{c}	39.2 ± 2.1^{c}	78.0 ± 1.4^{b}
170	2	17.2 ± 0.4^{b}	44.4 ± 1.4^{c}	423.4 ± 34.9^{a}	38.1 ± 1.5^{b}	35.5 ± 1.2^{b}	42.1 ± 1.2^{b}	81.3 ± 3.1^{b}
175	1.5	18.6 ± 0.4^{a}	52.6 ± 1.8^{a}	424.9 ± 32.5^{a}	52.6 ± 2.5^{a}	48.9 ± 2.6^{a}	55.5 ± 2.4^{a}	86.8 ± 3.4^{a}

X_1: temperature (°C), X_2: flow rate (mL/min), DPPH: 2,2-diphenyl-1-picrylhydrazyl, AAE: ascorbic acid equivalents, FRAP: ferric-reducing antioxidant power, FSE: ferrous sulfate equivalents, ORAC: oxygen radical absorbance capacity, TE: Trolox equivalents, ACE: angiotensin-I converting enzyme.

The same superscript letters in each column ($^{a-g}$) indicate no significant differences ($p < 0.05$).

Data are expressed as the mean ± standard deviation of triplicate experiments.

2.5. Correlations between flavonoid yields and biological properties of SW extracts

To determine which flavonoids affect the functional properties (antioxidant and enzyme—inhibitory activities) of the SW extracts, Pearson correlation coefficients (*r*-values) representing the associations between flavonoid yields and functional properties were calculated (Table 13). The sum of individual flavonoids was strongly correlated with DPPH radical scavenging activity (r = 0.911), FRAP (r = 0.798), and ORAC (r = 0.841), indicating that the total flavonoid content in the SW extracts has a large effect on antioxidant activities. The content of hesperidin, the major flavonoid in the peel, was also more strongly correlated with antioxidant activities (r = 0.725－0.857) compared to narirutin (r = 0.479－0.685). The sum of HHP contents (hesperetin-7-O-glucoside, hesperetin, prunin, and naringenin) was more strongly correlated with inhibitory activities against XO (r = 0.826), ACE (r = 0.798), α-glucosidase (r = 0.830), and PL (r = 0.795) than with antioxidant activities ($r \leq$ 0.719), indicating that HHP formed at high temperatures have a marked effect on enzyme inhibitory activities. Individual HHP were also more strongly correlated with inhibitory activities against XO ($r \geq$ 0.736), ACE ($r \geq$ 0.666), α-glucosidase ($r \geq$ 0.708), and PL ($r \geq$ 0.695) than were their precursors, hesperidin ($r \leq$ 0.602) and narirutin ($r \leq$ 0.393).

Table 13. Pearson correlation coefficients representing associations between flavonoid yields and biological activities.

	Antioxidant activity			Enzyme-inhibitory activity			
	DPPH radical scavenging activity	FRAP	ORAC	Xanthine oxidase	ACE	α-Glucosidase	Pancreatic lipase
Sum of all flavonoids	0.911**	0.798**	0.841**	0.615*	0.698*	0.647	0.676*
Sum of hydrolysis products	0.567	0.719*	0.629	0.826**	0.798**	0.830**	0.795*
Hesperidin (HPD)	0.857**	0.725*	0.782*	0.513	0.602	0.549	0.585
H7G (HPG)	0.505	0.651	0.576	0.796*	0.761*	0.793*	0.753*
Hesperetin (HPT)	0.629	0.786*	0.666	0.848**	0.831**	0.860**	0.830**
HPD+HPG+HPT	0.932**	0.822**	0.859**	0.639	0.719*	0.673*	0.702*
HPG+HPT	0.569	0.721	0.624	0.827**	0.801**	0.831**	0.796*
Narirutin (NRT)	0.685*	0.479	0.560	0.293	0.393	0.314	0.344
Prunin (PRN)	0.419	0.562	0.562	0.736*	0.666*	0.708*	0.695*
Naringenin (NGN)	0.664	0.812**	0.718*	0.845**	0.847**	0.887**	0.821**
NRT+PRN+NGN	0.786*	0.601	0.676*	0.432	0.526	0.453	0.477
PRN+NGN	0.543	0.692*	0.650	0.808**	0.768*	0.809**	0.773*
Sinensetin	0.459	0.269	0.292	0.047	0.139	0.029	0.102
Nobiletin	0.812**	0.696*	0.689*	0.518	0.591	0.520	0.571
Tangeretin	0.787*	0.625	0.690*	0.411	0.522	0.466	0.485
Total PMFs	0.782*	0.634	0.662	0.431	0.525	0.454	0.495

*$p < 0.05$ and **$p < 0.01$, sum of hydrolysis products: HPG+HPT+ PRN+NGN, DPPH: 2,2-diphenyl-1-picrylhydrazyl, FRAP: ferric-reducing antioxidant power, ORAC: oxygen radical absorbance capacity, ACE: angiotensin-I converting enzyme, PMFs: polymethoxyflavones.

2.6. Antioxidant activities of individual citrus flavonoids

Table 14 shows the antioxidant activities (DPPH, FRAP, and ORAC) of individual flavonoids. Hesperidin and its HHP exhibited 1.94－2.57-fold higher DPPH radical scavenging activity and 3.66－4.42-fold higher FRAP than did narirutin and its HHP, but there was no marked difference in ORAC. Mhiri et al. (2016) reported that the 2,2'-azinobis-(3-ethylbenzothiazoline-6-sulfonic acid) (ABTS) radical scavenging activity of hesperidin was 5.5-fold higher than that of narirutin due to the presence of a catechol group in the B-ring of the hesperidin molecule.

The antioxidant activities of monoglucosides (hesperetin-7-O-glucoside and prunin) and aglycones (hesperetin and naringenin) were high compared with those of diglucosides (hesperidin and narirutin), and among them, hesperetin exhibited the highest antioxidant activity. Flavonoid diglucosides exhibit lower antioxidant activities compared with their aglycones because one or more sugars are combined with aromatic hydroxyl groups in their molecular structures (Kumar and Pandey, 2013). PMFs did not exhibit DPPH radical scavenging activity and FRAP and exhibited a relatively low ORAC. Barreca et al. (2013) reported that PMFs in tangelo exhibited negligible antioxidant activities (DPPH radical scavenging activity, ABTS radical scavenging activity, FRAP, and hydroxyl radical scavenging activity).

Table 15 shows the theoretical antioxidant activities in the SW extracts calculated based on the antioxidant activities of individual flavonoids. All measured antioxidant activities were higher than the theoretical antioxidant activities in the SW extracts, which may have been due to the synergistic effects between flavonoids or unknown compounds produced under subcritical conditions. Plaza and Turner (2015) reported that new antioxidants were produced by Maillard, caramelization, and thermal oxidation reactions under subcritical conditions.

Table 14. Biological activities of individual citrus flavonoids.

	Antioxidant activity			Enzyme inhibitory activity (IC_{50})			
	DPPH radical scavenging activity (mg AAE/g)	FRAP (mmol FSE /100 g)	ORAC (mg TE/ 100 mg)	Xanthine oxidase (mg/L)	ACE (mg/L)	α-Glucosidase (mg/L)	Pancreatic lipase (mg/L)
Hesperidin	45.3 ± 0.9^{c}	399.7 ± 21.1^{c}	247.3 ± 13.2^{f}	> 2,000	1,375.8 ± 62.1^{b}	> 2,000	418.4 ± 21.7^{a}
Hesperetin-7-O-glucoside	51.6 ± 1.4^{b}	439.8 ± 18.4^{b}	323.9 ± 13.7^{d}	> 2,000	106.5 ± 3.8^{f}	1,395.5 ± 69.9^{b}	84.4 ± 4.2^{d}
Hesperetin	115.8 ± 3.9^{a}	549.1 ± 21.1^{a}	710.9 ± 12.0^{a}	275.4 ± 17.7^{c}	358.2 ± 7.8^{d}	131.8 ± 7.3^{e}	104.6 ± 5.2^{d}
Narirutin	17.6 ± 1.2^{e}	102.6 ± 4.1^{e}	283.4 ± 15.7^{e}	1,104.7 ± 40.7^{a}	1,937.1 ± 42.5^{a}	1,004.0 ± 42.6^{c}	> 2,000
Prunin	26.5 ± 0.2^{d}	99.5 ± 3.6^{e}	363.9 ± 18.1^{c}	862.5 ± 36.6^{b}	221.2 ± 6.2^{e}	622.7 ± 28.0^{d}	> 2,000
Naringenin	52.6 ± 3.3^{b}	150.3 ± 3.7^{d}	475.1 ± 13.3^{b}	129.3 ± 6.4^{d}	459.7 ± 15.0^{c}	72.2 ± 3.8^{e}	> 2,000
Sinensetin	N.D.	N.D.	7.6 ± 0.4^{g}	> 2,000	364.0 ± 13.4^{d}	> 2,000	301.4 ± 22.2^{b}
Nobiletin	N.D.	N.D.	6.0 ± 0.4^{g}	> 2,000	322.5 ± 4.7^{d}	> 2,000	426.4 ± 27.6^{a}
Tangeretin	N.D.	N.D.	5.8 ± 0.4^{g}	> 2,000	352.0 ± 8.9^{d}	1,763.1 ± 66.6^{a}	148.7 ± 6.5^{c}
Positive control				116.7 ± 3.7^{d} (Allopurinol)	6.9 ± 0.2^{g} (Captopril)	1,366.9 ± 73.2^{b} (Acarbose)	54.4 ± 3.6^{e} (Orlistat)

DPPH: 2,2-diphenyl-1-picrylhydrazyl, AAE: ascorbic acid equivalents, FRAP: ferric-reducing antioxidant power, FSE: ferrous sulfate equivalents, ORAC: oxygen radical absorbance capacity, TE: Trolox equivalents, ACE: angiotensin-I converting enzyme.

The same superscript letters in each column ($^{a-g}$) indicate no significant differences ($p < 0.05$). Data are expressed as the mean ± standard deviation of triplicate experiments.

Table 15. Theoretical and measured antioxidant activities in subcritical water extracts.

X_1	X_2	DPPH radical scavenging activity (mg AAE/g)		FRAP (mmol FSE/100 g)		ORAC (mg TE/g)	
		Theoretical	Measured	Theoretical	Measured	Theoretical	Measured
145	1.5	1.4	8.3 ± 0.1^{f}	11.9	24.7 ± 1.1^{f}	88.0	169.5 ± 5.2^{d}
150	1	1.2	8.2 ± 0.3^{f}	10.4	24.9 ± 0.9^{f}	76.5	122.8 ± 5.8^{e}
150	2	1.9	14.8 ± 0.5^{c}	16.0	28.9 ± 0.7^{e}	116.8	338.8 ± 16.6^{b}
160	0.75	1.3	9.5 ± 0.6^{e}	10.8	25.5 ± 0.9^{f}	80.4	281.3 ± 17.5^{c}
160	1.5	1.9	13.3 ± 0.7^{d}	16.3	45.3 ± 1.3^{c}	120.3	316.2 ± 26.3^{bc}
160	2.25	2.3	18.6 ± 0.3^{a}	19.3	48.8 ± 1.3^{b}	141.6	397.4 ± 21.8^{a}
170	1	1.8	14.0 ± 0.0^{cd}	14.4	39.3 ± 1.1^{d}	109.9	327.6 ± 5.0^{b}
170	2	2.2	17.2 ± 0.4^{b}	18.9	44.4 ± 1.4^{c}	139.6	423.4 ± 34.9^{a}
175	1.5	2.0	18.6 ± 0.4^{a}	16.5	52.6 ± 1.8^{a}	126.5	424.9 ± 32.5^{a}

X_1: temperature (°C), X_2: flow rate (mL/min), DPPH: 2,2-diphenyl-1-picrylhydrazyl, AAE: ascorbic acid equivalents, FRAP: ferric-reducing antioxidant power, FSE: ferrous sulfate equivalents, ORAC: oxygen radical absorbance capacity, TE: trolox equivalents.

The same superscript letters in each column ($^{a-f}$) indicate no significant differences ($p < 0.05$). Data are expressed as the mean ± standard deviation of triplicate experiments.

2.7. Biological activities of individual citrus flavonoids

The enzyme inhibitory activities of individual flavonoids were also measured (Tables 14). The inhibitory activities against XO and α-glucosidase exhibited by narirutin and its HHP were about twice those exhibited by hesperidin and its HHP due to the hydroxyl groups at the 4'-position of the B-ring in their molecules. The highest activities against both enzymes were exhibited by aglycones (hesperetin and naringenin), followed by monoglucosides (hesperetin-7-O-glucoside and prunin) and diglucosides (hesperidin and narirutin). In particular, naringenin exhibited a high inhibitory activity (IC_{50}) of 129.3 mg/L against XO, which was not significantly different from the value of 116.7 mg/L for the positive control, allopurinol. The inhibitory activity (IC_{50}) exhibited by naringen in against α-glucosidase was 72.2 mg/L, which was 18.9-fold higher than that (1,366.9 mg/L) of the positive control, acarbose. Yuan et al. (2019) reported that the inhibitory activities exhibited by flavonoids, such as kaempferol, quercetin, and naringenin, against XO decreased with increasing glycosylation. Hesperidin and its HHP exhibited relatively low inhibitory activities and PMFs exhibited almost no activities against XO and α-glucosidase due to the presence of methyl groups in their molecular structures. Lin et al. (2015) also reported that the methylation of hydroxyl groups at the B-ring of some flavonoids (luteolin and kaempferol) greatly reduced XO inhibitory activity.

The inhibitory activities against ACE were higher for hesperidin and its HHP than those for narirutin and its HHP, and those for monoglucosides and aglycones were 8.7－12.9-fold and 3.8－4.2-fold higher, respectively, than those for diglucosides. In particular, the ACE inhibitory activities exhibited by hesperetin-7-O-glucoside and prunin were the highest.

The inhibitory activity against PL was very high for hesperidin and its HHP, but very low for narirutin and its HHP. In particular, the inhibitory activities (IC_{50}) exhibited by hesperetin-7-O-glucoside and hesperetin were the highest (84.4 and 104.6 mg/L, respectively). This was due to a specific structure (methylation in the

4'-position) found in hesperidin and its HHP, which directly inhibits PL. Buchholz and Melzig (2015) also reported that the hydroxyl group at the 3'-position and the methyl group at the 4'-position of the B-ring in the hesperidin molecule favor inhibitory activity against PL. The SW extracts of citrus peel exhibited high inhibitory activities against PL probably due to the high content of hesperidin, which exhibits high inhibitory activity against PL (Table 12).

PMFs also exhibited relatively high inhibitory activities against ACE and PL due to methylation at the B-ring in their molecular structures. Kurita et al. (2010) reported that the O-methylated derivative of epigallocatechin gallate exhibited significant inhibitory activity against ACE. The inhibitory activity (IC_{50}) exhibited by tangeretin against PL was 148.7 mg/L, which was higher than those exhibited by sinensetin (301.4 mg/L) and nobiletin (426.4 mg/L). Structurally, sinensetin and nobiletin have two methyl groups at the 3'- and 4'- positions of the B-ring, whereas tangeretin has only one methyl group at the 4'-position (Fig. 1). Therefore, the methyl group at the 4'-position of the B-ring was assumed to play an important role in the inhibition of PL.

3. Conclusions

This study showed that 87.8%－98.9% of bioactive flavonoids (hesperidin, narirutin, sinensetin, nobiletin, and tangeretin) could be extracted from *Citrus unshiu* peel at 145.3－165.6 °C with a water flow rate of 2.25 mL/min in semi-continuous mode using water. Total flavonoid content in the SW extracts was strongly correlated with antioxidant activities (DPPH, FRAP, and ORAC), whereas the sum of HHP in the SW extracts was strongly correlated with inhibitory activities against XO, ACE, α-glucosidase, and PL. The highest antioxidant activities and enzyme inhibitory activities against XO and α-glucosidase were observed for aglycones (hesperetin and naringenin), whereas the highest enzyme inhibitory activities against ACE and PL were observed for monoglucosides of hesperetin and narirutin (i.e., hesperetin-7-O-glucoside and prunin). Therefore, hydrothermal hydrolysate-rich extracts could be used as a functional ingredient in nutraceutical, pharmaceutical, and medicinal industries. Further research on the eco-friendly SW hydrolysis process is required to convert flavonoid diglucosides from citrus peel to lower-molecular-weight compounds with higher functionality.

Part. Ⅲ

Subcritical Water Extraction and Hydrolysis of Flavonoids from Immature *Citrus unshiu* pomace

1. Materials and Methods

1.1. Sample preparation

Immature *Citrus unshiu* Markovich fruits were purchased from a local farm in Jeju, Korea. The fruits were rinsed, cut into quarters, and ground using a blender (Shinil Industrial Co., Ltd., Chungcheongnam-do, Republic of Korea) for 90 sec. The homogenates were pressed using a screw type juice extractor (Green Power, Daejeon, Republic of Korea) and the pomace was separated from the juice. The juice was filtered once again using gauze (pore size: 1 mm, Dae Han medical supply Co., Ltd., Chungcheongbuk-do, Republic of Korea) to recover the fine particles which were then combined with the pomace. The mixed pomace was freeze dried, crushed into the powders (14－50 mesh), and stored at －20 °C until further use.

1.2. Chemicals

Hesperidin and hesperetin were purchased from Sigma Chemical Co. (St. Louis, MO). Hesperetin-7-O-glucoside was purchased from Extrasynthese (Genay, France). Acetic acid was purchased from Junsei Chemical Co., Ltd (Chuo-ku, Tokyo, Japan) and HPLC grade acetonitrile and methyl alcohol were purchased from Daejung Chemicals & Metals Co., Ltd (Shiheung, Gyeonggi, Republic of Korea).

1.3. Subcritical water extraction and hydrolysis

SWE method of hesperidin from immature *Citrus unshiu* pomace (ICUP) is the same as in Part 1 except the followings. 0.5 g of ICUP was mixed with sea sand, and placed in the extractor. SW extracts were collected for 15 min. The effects of extraction temperature (150－170 °C) and flow rate (1－3 mL/min) on the yield of hesperidin were evaluated in the first oven. Under the optimum condition for

hesperidin extraction, subcritical water hydrolysis was further performed in the second oven (Fig. 10). The temperature (170－190 ℃) and the residence time (1.9－5.7 min) were evaluated on the hydrolysis yields of hesperetin-7-O-glucoside and hesperetin. The stainless steel tubing was used for hydrolysis coils (1/8 inch O.D., 3 －9 m length). The residence time (t, min) was calculated using the following equation (Lachos-Perez et al., 2020):

$$t = \frac{V_R p_R}{v_0 p_0} \tag{13}$$

where V_R is the volume of coils (m^3), v_0 is the water flow rate (mL/min), p_0 is the density of water at 25 ℃ and 5 MPa, and p_R is the density of the water at hydrolysis temperature and pressure.

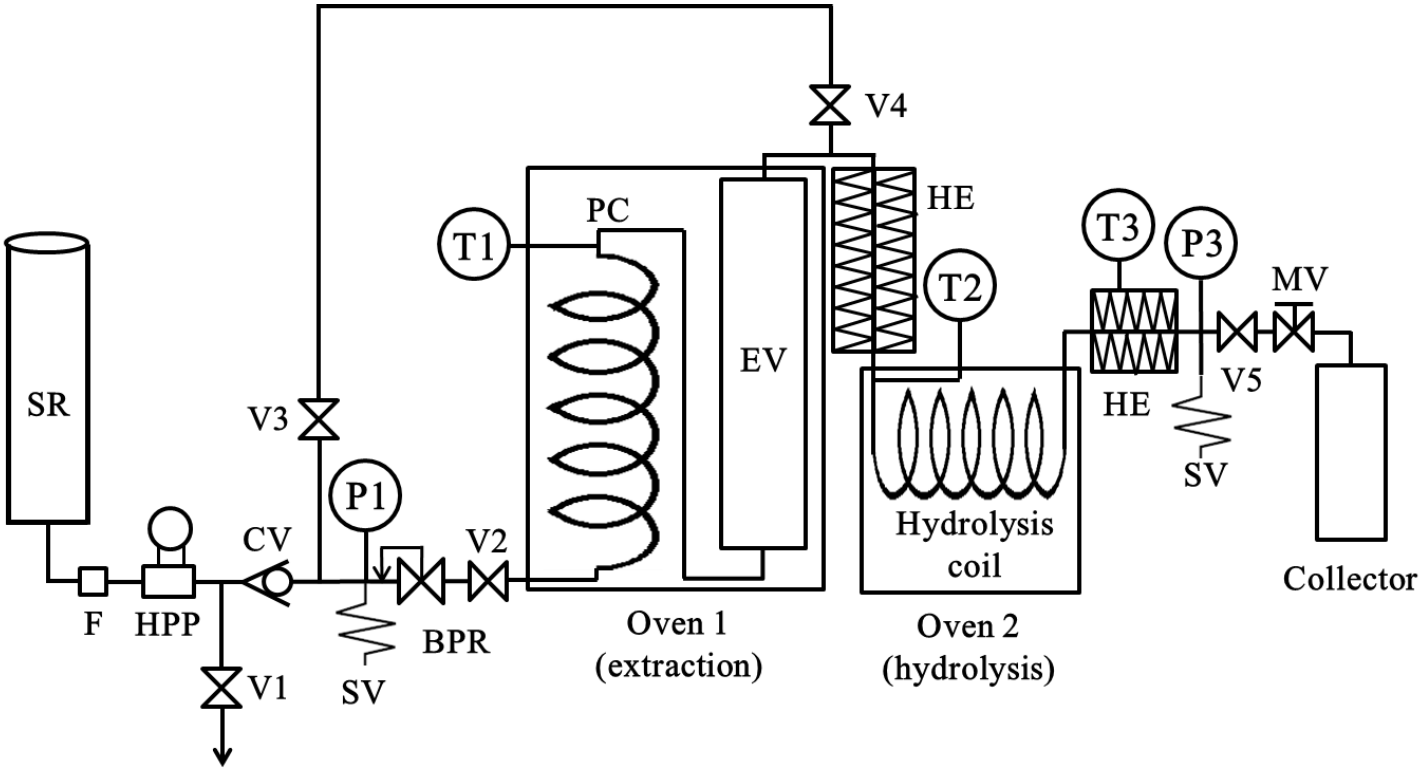

Fig. 10. Schematic diagram of semi-continuous subcritical water extraction and hydrolysis apparatus (CV: check valve, EV: extraction vessel, F: in-line filter, HE: heat exchanger, HPP: high pressure pump, MV: metering valve, P: pressure gauge, PC: preheating coil, PR: pressure regulator, SV: safety valve, SR: solvent reservoir, T: temperature indicator, V: on/off valve).

1.4. HPLC analysis

The same as in Parts 1 and 2.

1.5. Calculation of hydrolysis yield and loss of hesperidin

The hydrolysis yield (%) of hesperetin-7-O-glucoside or hesperetin was calculated according to the stoichiometry of the reaction using equation (14) (Ravber et al., 2015).

$$\text{Hydrolysis yield (μg/g dry sample)} = \frac{Q_C \times (MW_H/MW_C)}{Q_{H0}} \quad (14)$$

where Q_C is the quantity of the hydrolyzed product in SW hydrolysates (μg/g dry sample), Q_{H0} is the quantity of hesperidin in the raw sample (μg/g dry sample), MW_H and MW_C are molecular weights of hesperidin and hesperetin-7-O-glucoside or hesperetin, respectively.

The % loss of hesperidin during the hydrolysis reaction was calculated using the equation (15).

$$\text{Loss of hesperidin (\%)} = \left(\frac{Q_{H0} - (Q_H + Q_{H7G} + Q_{HT})}{Q_{H0}}\right) \times 100 \quad (15)$$

where Q_H is the quantity of the residual hesperidin in SW hydrolysates (μg/g dry sample), Q_{H7G} and Q_{HT} are the quantities of hesperetin-7-O-glucoside or hesperetin in SW hydrolysates (μg/g dry sample), respectively.

1.6. Response surface design

A face-centered central composite design was used to optimize the SWE of hesperidin yield, and SWH of hesperidin into hesperetin-7-O-glucoside and hesperetin, and %loss of hesperidin. Extraction temperature (X_1: 150－170 °C) and flow rate (X_2: 1－3 mL/min) are independent variables for SWE, and hydrolysis temperature (X_1: 170－190 °C) and residence time (X_2: 1.9－5.7 min) are independent variables for SWH. The quadratic polynomial (equation 6) was used to predict the optimal extraction conditions based on experimental data. The rest of them are the same as in Part 2.

2. Results and discussion

2.1. Composition of flavonoids in immature *Citrus unshiu* pomace

The flavonoid composition in the methanol extract of ICUP is shown in Table 16. The major flavonoids were hesperidin (49,731.5 μg/g dry sample) and narirutin (12,969.0 μg/g dry sample). The minor flavonoids were PMFs (0.22%) such as sinensetin (14.5 μg/ g dry sample), nobiletin (77.1 μg/g dry sample), and tangeretin (50.9. μg/g dry sample). The sum of all flavonoid contents was 62,843.0 μg/g dry sample.

Table 16. Composition of flavonoids in immature *Citrus unshiu* pomace.

Flavonoid	Content (μg/g dry sample)	(%)
Hesperidin	49,731.5 ± 808.51	79.1
Narirutin	12,969.0 ± 165.79	20.6
Sinensetin	14.5 ± 0.5	0.02
Nobiletin	77.1 ± 0.9	0.12
Tangeretin	50.9 ± 0.4	0.08
Total	62,843.0 ± 906.3	100

Data are expressed as the mean ± standard deviation of triplicate experiments.

2.2. Optimization of SWE

Table 17 presents the yields of hesperidin and its HHP (hesperetin-7-O-glucoside and hesperetin) in the SW extracts of ICUP at different extraction temperatures and flow rates. Table 18 presents the results of ANOVA and regression analysis for the hesperidin yield. The regression model provided good fits (R^2 = 0.9990, p-values < 0.05, lack-of-fit p-values > 0.05, differences between adjusted and predicted R^2 values < 0.2, %C.V. value 0.65%, and adequate precision 103.39)

The optimal extraction condition for maximizing the yield of hesperidin was estimated using the following second-order polynomial equations:

$$Y(\text{hesperidin}) = 39{,}926 - 1{,}219X_1 + 4{,}055X_2 - 7{,}089X_1^2 - 1{,}319X_2^2 + 1{,}057X_1X_2 \quad (16)$$

where Y is the hesperidin yield, X_1 is temperature, and X_2 is flow rate.

Based on the models, the optimal extraction temperature and flow rate for the maximum yield of hesperidin were 159.8 °C and 3.0 mL/min, respectively (Table 17). The predicted yield of hesperidin was 40,663 μg/g dry sample, which was 81.7% of the corresponding content in the raw material. The relationships between the hesperidin yield and extraction variables (temperature and flow rate) are presented in the response surface plots in Fig. 11.

Table 17. Face-centered central composite design and corresponding flavonoid yield in subcritical water extracts from immature *Citrus unshiu* pomace.

No	X_1	X_2	Hesperidin and its hydrolysis products (μg/g dry sample)			Sum of flavonoids (μg/g dry sample)
			Hesperidin	Hesperetin-7-O-glucoside	Hesperetin	
1	150	1	29,687	3,186	955	33,828
2	150	3	35,710	2,080	686	38,476
3	170	1	25,137	9,612	5,703	40,452
4	170	3	35,391	7,481	3,349	46,221
5	150	2	34,130	2,357	742	37,229
6	170	2	31,685	7,780	3,606	43,071
7	160	1	34,650	5,472	1,775	41,897
8	160	3	42,705	2,996	974	46,675
9	160	2	40,255	3,776	1,212	45,243
10	160	2	39,777	3,645	1,261	44,683
11	160	2	39,604	3,514	1,391	44,509

X_1: temperature (°C), X_2: flow rate (mL/min)

Table 18. Analysis of variance for regression model for SWE of hesperidin from immature *Citrus unshiu* pomace.

Source	Hesperidin	
	F-value	*p*-value
Model	1,021.4	< 0.0001
X_1	170.2	< 0.0001
X_2	1,883.7	< 0.0001
X_1^2	2,431.0	0.0003
X_2^2	84.2	< 0.0001
X_1X_2	85.4	0.0002
Lack of fit	0.1	0.9525
R^2	0.9990	
pred R^2	0.9975	
adj R^2	0.9980	
C.V%	0.65	
Adeq precision	103.3	

X_1: temperature (°C), X_2: flow rate (mL/min), pred R^2: predicted R^2, adj R^2: adjusted R^2, C.V: coefficient of variance, Adeq precision: adequate precision.

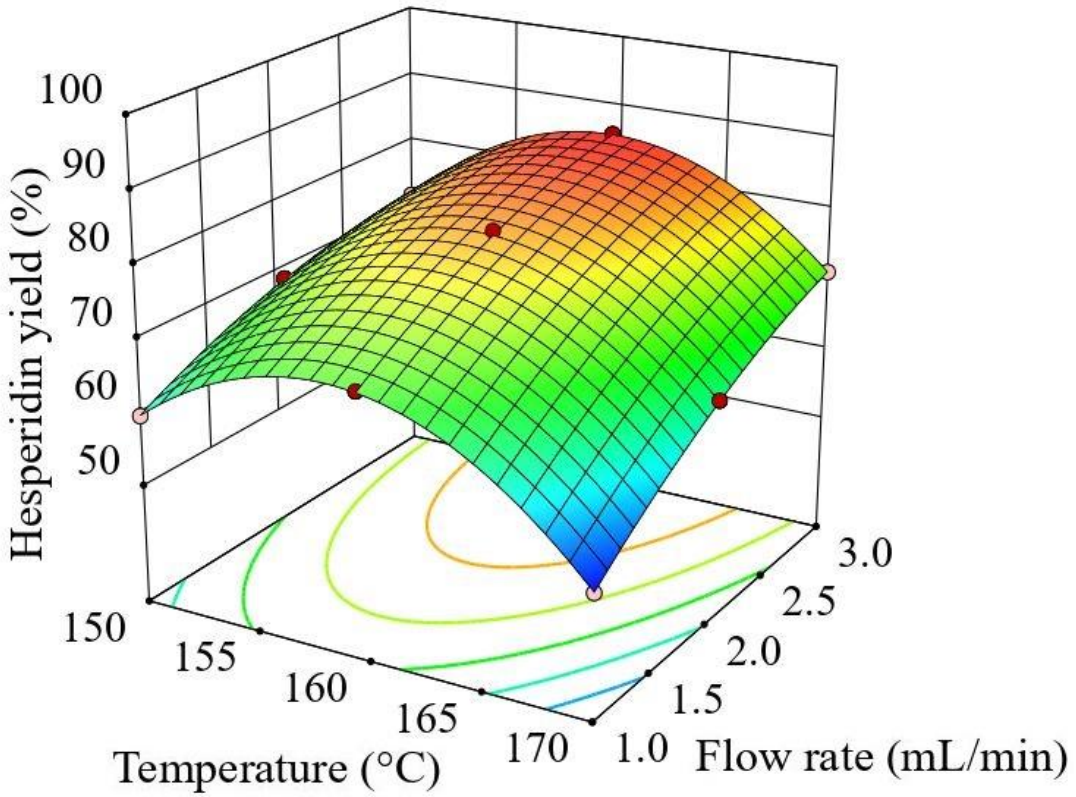

Fig. 11. Response surface plot indicating the effects of extraction temperature and flow rate on hesperidin yield.

2.3. Effects of extraction parameters

Table 17 and Fig. 11 present individual hesperidin and its hydrolysis products yields in the SW extracts of ICUP at different temperatures and flow rates. The hesperidin yield increased with increasing extraction temperature from 150 °C to 160 °C due to the decrease in dielectric constant as the temperature increased (Brunner, 2013; Céliz et al., 2015). However, the hesperidin yield decreased at 170 °C because hesperidin was rapidly hydrolyzed to hesperetin-7-O-glucoside or hesperetin (Ruen-ngam et al., 2012).

Table 17 and Fig. 11 also show the effects of water flow rates on the hesperidin yield. The yield of hesperidin increased significantly with an increasing flow rate from 1 to 3 mL/min due to the increased concentration gradient, superficial velocity, and mass transfer rate between the extraction solvent and the sample matrix at higher flow rate (Mottahedin et al., 2017; Kim and Lim, 2019). On the other hands, the low flow rate increases the residence time in the extraction vessel, causing a higher yields of hydrolysis products such as hesperetin-7-O-glucoside and hesperetin.

As shown in Table 17, The yield of hydrolysates produced in SWE of immature pomace was higher than that of mature peel (Table 8) because citric acid in immature pomace may act as a catalyst for the hydrolysis of hesperidin (Kang et al., 2005; Borges et al., 2011). Borges et al. (2011) reported that the content of total monomeric anthocyanins in water extract from *Euterpe edulis* pulp was increased with increasing citric acid concentrations (0.01－0.1 M).

2.4. Optimization of subcritical water hydrolysis

Table 19 presents the yields of hesperidin and its HHP (hesperetin-7-O-glucoside and hesperetin) in the SW hydrolysates of ICUP at different temperatures and residence times. The yields of hesperetin-7-O-glucoside and hesperetin, and %loss of hesperidin were selected as the responses for optimization of hydrolysis condition because the hesperidin is the major flavonoid in ICUP and has high enzyme inhibitory activities against pancreatic lipase (weight control effect).

Table 20 presents the results of ANOVA and regression analysis. All regression models provided good fits (R^2 > 0.9629, p-values < 0.05, lack-of-fit p-values > 0.05, differences between adjusted and predicted R^2 values < 0.2, and adequate precision > 14). On the other hands, the %C.V. in the %loss of hesperidin was 28.7% due to the large error at the center points with the low loss values.

The optimal extraction conditions for maximizing the yields of hesperetin-7-O-glucoside (H7G) and hesperetin, and minimizing loss of hesperidin were estimated using the following second-order polynomial equations:

$$Y\ (\mathrm{H7G}) = 11{,}474 + 823X_1 + 56.2X_2 - 2{,}310X_1^2 - 591X_2^2 - 558X_1X_2 \quad (17)$$

$$Y\ (\mathrm{hesperetin}) = 7{,}592 + 2{,}812X_1 + 1{,}001X_2 - 681X_1^2 - 193X_2^2 + 99.7X_1X_2 \quad (18)$$

$$Y\ (\mathrm{Loss\ of\ hesperidin}) = 97.9 - 3.39X_1 - 2.80X_2 - 3.32X_1^2 - 0.0538X_2^2 - 2.00X_1X_2 \quad (19)$$

where Y is the responses, X_1 is temperature, and X_2 is residence time.

Based on the models, the optimal hydrolysis conditions for maximum production of hesperetin-7-O-glucoside and hesperetin were 181.8 °C, 3.7 min and 189.6 °C, 5.6 min, respectively, and the condition for minimizing the loss of hesperidin was 174.4 °C, 2.0 min (Table 21). The predicted yields of hesperetin-7-O-glucoside and hesperetin were 11,548 and 10,533 μg/g dry sample, respectively, and predicted values of %loss of hesperidin was −0.2%. The optimal SWH condition for

simultaneous production of hesperetin-7-O-glucoside and hesperetin with minimizing the loss of hesperidin was temperature of 182.8 °C and residence time of 3.2 min. The predicted yields of hesperetin-7-O-glucoside and hesperetin at simultaneous optimum conditions were 11,499 and 8,029 μg/g dry sample, respectively, and the loss of hesperidin was only 2.3%. The relationships between the responses (hesperetin-7-O-glucoside and hesperetin yields, and loss of hesperidin) and experimental variables (hydrolysis temperature and residence time) are presented in the response surface plots in Fig. 12.

Table 19. Face-centred central composite design and corresponding flavonoid yield in subcritical water hydrolysates from immature *Citrus unshiu* pomace.

No	X_1	X_2	Hesperidin and its hydrolysis products (μg/g dry sample)			Sum of hydrolysates (μg/g dry sample)	Sum of flavonoids (μg/g dry sample)
			Hesperidin	Hesperetin-7-O-glucoside	Hesperetin		
1	170	1.9	33,291	7,251	3,247	10,498	43,789
2	170	5.7	27,710	8,430	4,657	13,087	40,797
3	190	1.9	17,187	10,116	8,726	18,842	36,029
4	190	5.7	9,753	9,061	10,535	19,596	29,349
5	170	3.8	29,793	8,159	4,003	12,162	41,955
6	190	3.8	13,161	9,601	9,519	19,120	32,281
7	180	1.9	23,814	10,492	5,854	16,346	40,160
8	180	5.7	15,901	10,705	8,642	19,347	35,248
9	180	3.8	17,097	11,957	7,905	19,862	36,959
10	180	3.8	18,532	11,295	7,418	18,713	37,245
11	180	3.8	18,403	11,737	7,752	19,489	37,892

X_1: temperature (°C), X_2: residence time (min)

Table 20. Analysis of variance for regression models for SWH of hesperidin from immature *Citrus unshiu* pomace.

Source	Hesperetin-7-O-glucoside		Hesperetin		Loss of hesperidin	
	F-value	*p*-value	*F*-value	*p*-value	*F*-value	*p*-value
Model	29.3	0.0010	74.7	0.0001	25.9	0.0014
X_1	16.1	0.0037	321.8	< 0.0001	55.1	0.0007
X_2	0.12	0.7411	40.8	0.0014	37.5	0.0017
X_1^2	87.0	0.0002	7.97	0.0371	22.3	0.0052
X_2^2	5.70	0.0626	0.64	0.4578	0.0059	0.9420
X_1X_2	8.04	0.0365	0.26	0.6256	12.8	0.0158
Lack of fit	1.61	0.4058	3.29	0.2416	0.92	0.5566
R^2	0.9671		0.9868		0.9629	
pred R^2	0.8194		0.8892		0.7801	
adj R^2	0.9342		0.9736		0.9258	
C.V%	3.99		5.40		28.7	
Adeq precision	14.9		26.8		17.3	

X_1: temperature (°C), X_2: residence time (min), pred R^2: predicted R^2, adj R^2: adjusted R^2, C.V: coefficient of variance, Adeq precision: adequate precision.

Table 21. Subcritical water hydrolysis parameters for maximizing yield of hesperetin-7-O-glucoside and hesperetin, and minimizing loss of hespeidin from immature *Citrus unshiu* pomace.

	Temperature (°C)	Residence time (min)	Predicted yield (μg/g dry sample)	Hydrolysis yield (%)	Desirability
Hesperetin-7-O-glucoside (H7G)	181.8	3.7	11,548	30.5	0.913
Hesperetin (HT)	189.7	5.6	10,533	42.8	1.000
Loss of hesperidin (LOH)	174.4	2.0	−0.2%	−0.2%	1.000
H7G+HT+LOH	182.8	3.2	11,499.6/ 8,030.1/ 2.3%	30.4/ 32.6	0.799

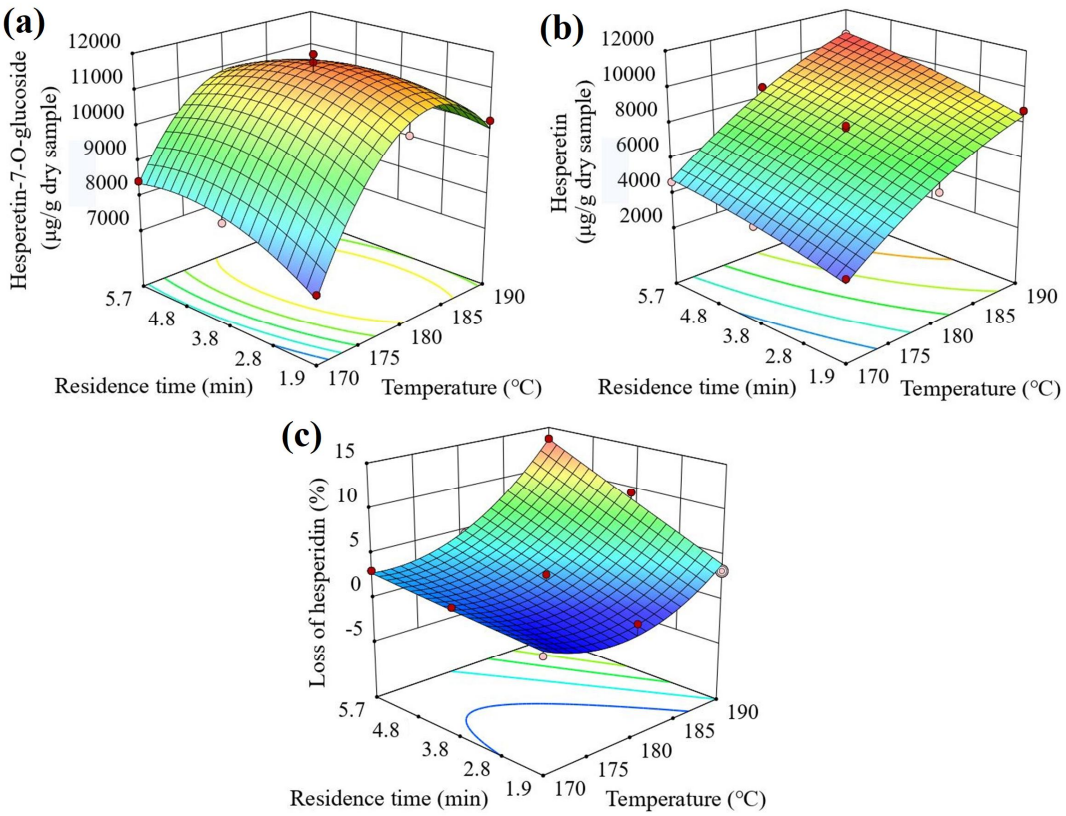

Fig. 12. Response surface plots indicating the effects of hydrolysis temperature and residence time on yields of (a) hesperetin-7-O-glucoside, (b) hesperetin, and (c) loss of hesperidin.

2.5. Effects of hydrolysis parameters

Table 19 presents yields of hesperidin and its HHP (hesperetin-7-O-glucoside and hesperetin) in the SW hydrolysates of ICUP at different temperatures and residence times. Hydrolysis temperature was a more important factor than residence time in hydrolysis of hesperidin. The yield of hesperetin-7-O-glucoside was greatly increased as the increase in temperature from 170 °C to 180 °C and then decreased at 190 °C (Fig. 12a). Water has high ionic products at high temperature, providing an acidic medium for the hydrolysis reaction, thereby increasing the hydrolysis of hesperidin into hesperetin-7-O-glucoside (Shitu et al., 2015). On the other hands, the high temperature hydrolyzes hesperetin-7-O-glucoside further to aglycone (hesperetin) (Ruen-ngam et al., 2012). The effect of residence time on hesperetin-7-O-glucoside yield was different depending on the hydrolysis temperature. The yield of hesperetin-7-O-glucoside increased with increasing the residence time at 170 °C, but decreased with increasing the residence time at 190 °C. Baig et al. (2013) reported that the conversion yield of sunflower oil by SW hydrolysis was gradually increased with increasing residence time from 20 to 100 min at 270 °C, however, conversion yields at 310 °C was about 90% at residence time of 45 min, and decreased at the residence time above that. Therefore, in order to enhance the production of hesperetin-7-O-glucoside using SWH, hesperidin should be hydrolyzed at high temperature with short residence time or at low temperature with long residence time.

Fig. 12b present the response surface plots for the effect of hydrolysis parameters on the yield of hesperetin. The yield of hesperetin significantly increased as the hydrolysis temperature increased from 170 °C to 190 °C because the hesperidin and hesperetin-7-O-glucoside were hydrolyzed to hesperetin. With increasing the residence time, the yield of hesperetin was slightly increased at all hydrolysis temperatures. Kim and Lim (2017) reported that SW temperature had a significant effect on the hydrolysis of rutin into quercetin, and the yield of quercetin was increased up to 180 °C.

Fig. 12c present the response surface plot for the loss of hesperidin. The loss of hesperidin did not occur at a hydrolysis temperature below 180 ℃, but increased rapidly when the temperature increased to 180－190 ℃. The loss of hesperidin also did not occur when the residence time increased at a temperature below 180 ℃, but the loss of hesperidin increased rapidly as the residence time increased. This is because the produced hesperetin from hesperidin and hesperetin-7-O-glucoside was decomposed into smaller compounds at high temperature with long residence time conditions. Ravber et al. (2016) reported that quercetin, produced by SW hydrolysis of rutin, was degraded into fragmentation compounds such as protocatechuic acid and catechol at high temperature.

3. Conclusion

Hesperidin in SW extract has been hydrolyzed by subcritical water. The response surface methodology was used to optimize the effects of the hydrolysis temperature and residence time for hydrolysis of hesperidin to valuable compounds, hesperetin-7-O-glucoside and hesperetin. The optimum condition for maximum production of hesperetin-7-O-glucoside and hesperetin with minimum loss of hesperidin simultaneously was temperature of 182.8 °C, and residence time of 3.2 min, where the predicted maximum yields of hesperetin-7-O-glucoside and hesperetin were 11,499 and 8,030 μg/g dry sample, respectively. Temperature was an important factor in SWH of hesperidin. The effect of residence time on hydrolysis was dependent on the hydrolysis temperature, and short residence time was required at high temperature. In this study, we identified the possibility of the successive conversion of hesperidin to valuable compounds within short time using an environmentally friendly solvent (water).

국문요약

감귤 껍질에는 flavanone으로서 hesperidin과 narirutin이 다량 함유되어 있으며, polymethoxyflavones(PMFs)로서 sinensetin, nobiletin, tangeretin이 소량 함유되어 있는데, 이들 성분은 항산화, 항염, 항암, 심장 보호 등의 기능성을 나타낸다. 제1부에서는 아임계수를 이용하여 온주밀감 껍질로부터 플라보노이드를 여러 온도(120－180 °C)와 유속(1.0－2.0 mL/min)에서 추출하여 추출기작을 밝혀내었다. Hesperidin, narirutin, PMFs의 추출수율은 120 °C에서 40.9%, 69.0%, 67.4%이었으며, 추출온도를 160 °C로 증가시키면 79.6%, 81.9%, 89.0%로 증가하였으나, 추출온도 180 °C에서는 열분해되어 감소하였다. 물의 유속 1.0－2.0 mL/min에서의 추출 곡선을 thermodynamic partitioning과 kinetic desorption 모델에 적용하여 추출기작을 예측하였다. 추출 속도는 추출 초기 단계에서는 빨랐지만 후기 단계에서는 느렸다. Thermodynamic partitioning 모델은 추출 초기에는 추출속도를 잘 예측할 수 있었으나 추출 후반부에는 잘 예측하지 못하였다. 반면 two-site kinetic desorption 모델은 추출 전반부 뿐만 아니라 후반부에서도 추출 속도를 매우 예측할 수 있었으며, 이로부터 감귤 껍질로부터 플라보노이드의 추출은 주로 입자 내 확산에 의해 이루어진다는 것을 알 수 있었다. 또한 two-site kinetic desorption 모델은 열분해되는 온도(180 °C)에서도 추출속도를 잘 예측할 수 있었던 것으로 보아, 이 모델은 아임계수를 이용한 감귤 플라보노이드의 추출은 물론 분해 기작을 모두 잘 설명 할 수 있었다. Hesperidin의 확산계수는 120 °C, 1 mL/min에서보다 160 °C, 2 mL/min에서 약 9.8배 높았다. Hesperidin의 확산에 필요한 활성화 에너지(37.2－43.8 kJ/mol)는 narirutin과 PMFs의 활성화 에너지(8.2－36.8 kJ/mol)보다 높았다. 따라서 감귤 껍질로부터 플라보노이드의 추출은 주로 입자 내 확산에 의해 이루어졌으며, 환경 친화적인 용매인 물을 사용하여 단시간 내에 추출할 수 있음을 보여주었다.

제2부에서는 아임계수를 사용하여 감귤 껍질로부터 플라보노이드를 추출과 가수분해하였고, 아임계수 추출물의 개별 플라보노이드의 수율, 항산화 활성 및 효소 억제 활성을 측정하였다. Hesperidin과 narirutin의 추출수율은 추출온도가 145

°C에서 165 °C로 증가함에 따라 증가하였다. 제1배당체(hesperetin-7-O-glucoside, prunin), 비배당체(hesperetin, naringenin)와 같은 가수분해물은 160 °C 이상의 온도에서 생성되었다. 아임계수 추출물에서 hesperidin, hesperetin-7-O-glucoside, hesperetin 함량은 항산화 활성과 밀접한 관련이 있는 반면, hesperetin과 naringenin의 함량은 효소 억제 활성과 밀접한 관련이 있었다. Hesperetin은 가장 높은 항산화 활성을 보인 반면, hesperetin-7-O-glucoside는 angiotensin-I converting enzyme(ACE)과 pancreatic lipase(PL)에 대한 강한 저해 활성을 나타내었다. Naringenin은 xanthine oxidase와 α-glucosidase에 대한 강한 저해 활성을 나타내었다. PMFs도 ACE와 PL에 대해 상대적으로 높은 저해 활성을 나타내었다. 따라서 친환경 용매인 물을 이용하여 짧은 시간 내에 감귤 껍질로부터 생리활성이 높은 플라보노이드를 추출 및 가수 분해할 수 있음을 확인하였다.

제3부에서는 감귤 미숙과 착즙박을 대상으로 반연속식 아임계수 추출 및 가수분해 장치을 이용하여 아임계수 추출물 중의 hesperidin을 생리활성이 높은 hesperetin-7-O-glucoside와 hesperetin으로 가수분해하였다. Hesperidin의 손실을 최소화하면서 동시에 hesperetin-7-O-glucoside와 hesperetin의 생성을 극대화하기 위한 최적조건은 가수분해 온도 182.8 °C와 체류시간 3.2분이었으며, 위 조건에서 hesperetin-7-O-glucoside와 hesperetin의 생성량은 각각 11,499와 8,030 μg/g dry sample이었다. 처리 온도는 hesperidin의 아임계수 가수분해에 있어서 가장 중요한 요소였다. 체류시간이 가수분해에 미치는 영향은 온도에 따라 달랐으며, 고온의 가수분해 조건에서는 짧은 체류 시간이 요구되었다. 따라서 환경 친화적 용매인 물을 사용하여 짧은 시간 내에 hesperidin을 기능성이 높은 물질로 연속적으로 전환할 수 있는 가능성을 확인하였다.

References

Al-Hamimi S, Mayoral AA, Cunico LP, Turner C. 2016. Carbon dioxide expanded ethanol extraction: solubility and extraction kinetics of α-pinene and cis-verbenol. Anal. Chem. 88, 4336-4345.

Amaretti A, Raimondi S, Leonardi A, Quartieri A, Rossi M. 2015. Hydrolysis of the rutinose-conjugates flavonoids rutin and hesperidin by the gut microbiota and bifidobacteria. Nutrients 7, 2788-2800.

An HJ, Park KJ, Kim SS. 2017. Flavonoids composition and antioxidant activity of by-products of five orange cultivars during maturation. Korean J. Food Preserv. 23, 1012-1017.

Andujar SA, Filippa MA, Ferretti FH, Blanco SE. 2003. Isomerization of 4'-methoxy-flavanone in alkaline medium. Determination of the enolate formation constant. Theochem. J. Mol. Struct. 636, 157-166.

Anekpankul T, Goto M, Sasaki M, Pavasant P, Shotipruk A. 2007. Extraction of anti-cancer damnacanthal from roots of *Morinda citrifolia* by subcritical water. Sep. Purif. Technol. 55, 343-349.

Asl AH, Khajenoori M. 2013. Subcritical water extraction, in: H. Nakajima (Ed.), Mass Transfer — Advances in Sustainable Energy and Environment Oriented Numerical Modeling. InTech, Rijeka, p. 464-466, 469.

Baig MN, Santos RCD, King J, Pioch D, Bowra S. 2013. Evaluation and modelling of continuous flow sub-critical water hydrolysis of biomass derived components; lipids and carbohydrates. Chem. Eng. Res. Des. 91, 2663–2670.

Barba FJ, Zhu Z, Koubaa M, Sant'Ana AS, Orlien V. 2016. Green alternative methods for the extraction of antioxidant bioactive compounds from winery wastes and by-products: A review, Trends Food Sci. Technol. 49, 96-109.

Barreca D, Bisignano C, Ginestra G, Bisignano G, Bellocco E, Leuzzi U, Gattuso G. 2013. C- and O-glycosyl flavonoids in tangelo (*Citrus reticulata* × *Citrus paradisi*) juice and their influence on antioxidant properties. Food Chem. 141, 1481-1488.

Barrera Vázquez MF, Comini LR, Milanesio JM, Núnez Montoya SC, Cabrera JL, Bottini S, Martini RE. 2015. Pressurized hot water extraction of anthraquinones from *Heterophyllaea pustulat*a Hook f. (Rubiaceae). J. Supercrit. Fluids 101, 170-175.

Borges GDSC, Vieira FGK, Copetti C, Gonzaga LV, Fett R. 2011. Optimization of the extraction of flavonols and anthocyanins from the fruit pulp of *Euterpe edulis* using response surface methodology. Food Res. Int. 44, 708-715.

Brunner G. 2014. Hydrothermal and Supercritical Water Process. in: D. Kiran (Ed.), Elsevier, Amsterdam, p. 71, 77, 84.

Buchholz T, Melzig MF. 2015. Polyphenolic compounds as pancreatic lipase inhibitors. Planta Med. 81, 771-783.

Burke AC, Sutherland BG, Telford DE, Morrow MR, Sawyez CG, Edwards JY, Drangova M, Huff MW. 2018. Intervention with citrus flavonoids reverses obesity and improves metabolic syndrome and atherosclerosis in obese Ldlr－/－ mice. J. Lipid Res. 59, 1714-1728.

Cacace JE, Mazza G. 2003. Mass transfer process during extraction of phenolic compounds from milled berries. J. Food Eng. 59, 379-389.

Cheigh CI, Chung EY, Chung MS. 2012. Enhanced extraction of flavanones hesperidin and narirutin from *Citrus unshiu* peel using subcritical water. J. Food Eng. 110, 472-477.

Céliz G, Rodriguez G, Soria F, Daz M. 2014. Synthesis of hesperetin7-O-glucoside from flavonoids extracted from citrus waste using both free and immobilized α -L-rhamnosidases. Biocatal. Agric. Biotechnol. 4, 335-341.

Chen PX, Tang Y, Marcone MF, Pauls PK, Zhang B, Liu R, Tsao R. 2015. Characterization of free, conjugated and bound phenolics and lipophilic antioxidants in regular- and non-darkening cranberry beans (*Phaseolus vulgaris* L.). Food Chem. 185, 298-308.

Dominguez H, Munoz MJG. 2017. Water extraction of bioactive compounds: from plants to drug development. Elsevier, Amsterdam, p. 19.

Duba KS, Casazza AA, Mohamed HB, Perego P, Fiori L. 2015. Extraction of polyphenols from grape skins and defatted grape seeds using subcritical water: experiments and modeling. Food Bioprod. Process. 94, 29-38.

Gabriele M, Frassinetti S, Caltavuturo L, Montero L, Dinelli G, Longo V, Gioia DD, Pucci L. 2017. Citrus bergamia powder: antioxidant, antimicrobial and anti-inflammatory properties. J. Funct. Foods 31, 255-265.

Gbashi S, Adebo OA, Piater L, Madala NE, Njobeh PB. 2016. Subcritical water extraction of biological materials. Sep. Purif. Rev. 46, 21-34.

Gil-Izquierdo A, Gil MI, Ferreres F. 2002. Effect of processing techniques at industrial scale on orange juice antioxidant and beneficial health compounds. J. Agric. Food Chem. 50, 5107-5114.

Gironés-Vilaplana A, Moreno DA, García-Viguera C. 2014. Phytochemistry and biological activity of Spanish Citrus fruits. Food Funct. 5, 764-772.

Ho CHL, Cacace JE, Mazza G. 2008. Mass transfer during pressurized low polarity water extraction of lignans from flaxseed meal. J. Food Eng. 89, 64-71.

Hussain F, Jahan N, Rahman K, Sultana B, Jamil A. 2018. Identification of hypotensive biofunctional compounds of *Coriandrum sativum* and evaluation of their angiotensin-converting enzyme (ACE) inhibition potential. Oxidative Med. Cell. Longev. 2018, 4643736.

Islam MN, Jo YT, Jung SK, Park JH. 2013. Thermodynamic and kinetic study for subcritical water extraction of PAHs. J. Ind. Eng. Chem. 19, 129-136.

Kang YJ, Yang MH, Ko WJ, Park SR, Lee BG. 2005. Studies on the major components and antioxidative properties of whole fruit powder and juice prepared from premature mandarin orange. Korean J. Food Sci. Technol. 37, 783-788.

Kanmaz EO, Saral O. 2017. The effect of extraction parameters on antioxidant activity of subcritical water extracts obtained from mandarin peel. Gida. 42, 405–412.

Kim JW, Mazza G. 2007. Mass transfer during pressurized low-polarity water extraction of phenolics and carbohydrates from flax shives, Ind. Eng. Chem. Res. 46, 7221-7230.

Kim YM, Lee EW, Eom SH, Kim TH. 2014. Pancreatic lipase inhibitory stilbenoids from the roots of *Vitis vinifera*. Int. J. Food Sci. Nutr. 65, 97-100.

Kim DS, Lim SB. 2017. Optimization of subcritical water hydrolysis of rutin into isoquercetin and quercetin. Prev. Nutr. Food Sci. 22, 131-137.

Kim SH, Park HJ, Kim KJ, Kim MJ, Lee JA, Lee AR, Roh SS. 2018a. Antioxidant activity of citrus peel and effect on its glucose metabolism in L6 rat skeletal muscle cells. Kor. J. Herbol. 33, 101-108.

Kim MY, Choi EO, Bo HH, Kwon DH, Ahn KI, Kim HJ, Ji SY, Hong SH, Jeong JW, Kim GY, Park C, Choi YH. 2018b. Reactive oxygen species-dependent apoptosis induction by water extract of *Citrus unshiu* peel in MDA-MB-231 human breast carcinoma cells. Nutr. Res. Pract. 12, 129-134.

Kim MY, Bo HH, Ji SY, Hong SH, Choi SH, Kim SO, Park C, Choi YH. 2019. Relationship between reactive oxygen species and adenosine monophosphate-activated protein kinase signaling in apoptosis induction of human breast adenocarcinoma

MDA-MB-231 cells by ethanol extract of *Citrus unshiu* peel. J. Life Sci. 29, 410-420.

Kim DS, Lim SB. 2019. Subcritical water extraction of rutin from the aerial parts of common buckwheat. J. Supercrit. Fluids 152, 104561.

Khajenoori M, Asl AH, Hormozi F. 2009. Proposed models for subcritical water extraction of essential oils. Chin. J. Chem. Eng. 17, 359-365.

Kubátová A, Jansen B, Vaudoisot JF, Hawthorne SB. 2002. Thermodynamic and kinetic models for the extraction of essential oil from savory and polycyclic aromatic hydrocarbons from soil with hot (subcritical) water and supercritical CO_2, J. Chromatogr. A 975, 175-188.

Kumar S, Pandey AK. 2013. Chemistry and biological activities of flavonoids: An overview. Sci. World J. 2013, 162750.

Kurita I, Maeda-Yamamoto M, Tachibana H, Kamei M. 2010. Antihypertensive effect of benifuuki tea containing O-methylated EGCG. J Agric Food Chem. 58, 1903-1908.

Lachos-Perez D, Baseggio AM, Mayanga-Torres PC, Junior MRM, Rostagno MA, Martínez J, Forster-Carneiro T. 2018. Subcritical water extraction of flavanones from defatted orange peel. J. Supercrit. Fluids 138, 7-16.

Lachos-Perez D, Baseggio AM, Torres-Mayanga PC, Ávila PF, Tompsett GA, Marostica M, Goldbeck R, Timko MT, Rostagno M, Martinez J, Forster-Carneiro T. 2020. Sequential subcritical water process applied to orange peel for therecovery flavanones and sugars. J. Supercrit. Fluids 160, 104789.

Lai CS, Wu JC, Ho CT, Pan MH. 2015. Disease chemopreventive effects and molecular mechanisms of hydroxylated polymethoxyflavones. BioFactors 41, 301-313.

Lin S, Zhang G, Liao Y, Pan J, Gong D. 2015. Dietary flavonoids as xanthine oxidase inhibitors: Structure-affinity and structure-activity relationships. J. Agric. Food

Chem. 63, 7784-7794.

Mehmood B, Dar KK, Ali S, Awan UA, Nayyer AQ, Ghous T, Andleeb S. 2015. *In vitro* assessment of antioxidant, antibacterial and phytochemical analysis of peel of *Citrus sinensis.* Pak. J. Pharm. Sci. 28, 231-239.

Mhiri N, Veys-Renaux D, Rocca E, Ioannou I, Boudhrioua NM, Ghoula M. 2016. Corrosion inhibition of carbon steel in acidic medium by orange peel extract and its main antioxidant compounds. Corrosion Sci. 102, 55-62.

Mortazavi SV, Eikani MH, Mirzaei H, Jafari M, Golmohammad F. 2010. Extraction of essential oils from *Bunium persicum* Boiss. using superheated water. Food Bioprod. Process. 88, 222-226.

Mottahedin P, Asl AH, Khajenoori M. 2017. Extraction of curcumin and essential oil from *Curcuma longa* L. by subcritical water via response surface methodology. J. Food Process. Preserv. 41, e13095.

Nastic N, Svarc-Gajic J, Delerue-Matos C, Morais S, Barroso MF, Moreira MM. 2018. Subcritical water extraction of antioxidants from mountain germander (*Teucrium montanum* L.). J. Supercrit. Fluids 138, 200-206.

Nile SH, Nile A, Gansukh E, Baskar V, Kai G. 2019. Subcritical water extraction of withanosides and withanolides from ashwagandha (*Withania somnifera* L) and their biological activities. Food Chem. Toxicol. 132, 110659.

Nipornram S, Tochampa W, Rattanatraiwong P, Singanusong R. 2018. Optimization of low power ultrasound-assisted extraction of phenolic compounds from mandarin (*Citrus reticulata* Blanco cv. Sainampueng) peel. Food Chem. 1, 338-345.

Park HY, Park Y, Lee Y, Noh SK, Sung EG, Choi I. 2012. Effect of oral administration of water-soluble extract from citrus peel (*Citrus unshiu*) on suppressing alcohol-induced fatty liver in rats. Food Chem. 130, 598-604.

Peng H, Li W, Li H, Deng Z, Zhang B. 2018. Extractable and non-extractable bound phenolic compositions and their antioxidant properties in seed coat and cotyledon of black soybean (Glycinemax (L.) merr). J. Funct. Food 32, 296-312.

Plaza M, Turner C. 2015. Pressurized hot water extraction of bioactives, Trends Anal. Chem. 71, 39-54.

Proenca C, Freitas M, Ribeiro D, Oliveira EFT, Sousa JLC, Tome SM, Ramos MJ, Silva AMS, Fernandes PA, Fernandes E. 2017. α-Glucosidase inhibition by flavonoids: An *in vitro* and *in silico* structure-activity relationship study. J. Enzym. Inhib. Med. Chem. 32, 1216-1228.

Rafiq S, Kaul R, Sofi SA, Bashir N, Nazir F, Nayik GA. 2018. Citrus peel as a source of functional ingredient: A review. J. Saudi Soc. Agric. Sci. 17, 351-358.

Ravber M, Knez Z, Škerget M. 2015. Optimization of hydrolysis of rutin in subcritical water using response surface methodology. J. Supercrit. Fluids 104, 145-152.

Ravber M, Pečar D, Goršek A, Iskra J, Knez Ž, Škerget M. 2016. Hydrothermal degradation of rutin: Identification of degradation products and kinetics study. J. Agric. Food Chem. 64, 9196－9202.

Revathy J, Srinivasan S, Abdullah SHS, Muruganathan U. 2018. Antihyperglycemic effect of hesperetin, a citrus flavonoid, extenuates hyperglycemia and exploring the potential role in antioxidant and antihyperlipidemic in streptozotocin-induced diabetic rats. Biomed. Pharmacother. 97, 98-106.

Richter BE, Jones BA, Ezzell JL, Porter NL. 1996. Accelerated solvent extraction: a technique for sample preparation. Anal. Chem. 68, 1033-1039.

Ruen-ngam D, Quitain AT, Tanaka M, Sasaki M, Goto M. 2012. Reaction kinetics of hydrothermal hydrolysis of hesperidin into more valuable compounds under

supercritical carbon dioxide conditions. J. Supercrit. Fluids 66, 215-220.

Sarfarazi M, Jafari SM, Rajabzadeh G, Feizi J. 2019. Development of an environmentally-friendly solvent-free extraction of saffron bioactives using subcritical water. LWT-Food Sci. Technol. 114, 108428.

Sengers JV, Watson JTR. 1986. Improved international formulations for the viscosity and thermal conductivity of water substance. J. Phys. Chem. Ref. Data 15, 1291-1314.

Shabkhiz MA, Eikani MH, Sadr ZB, Golmohammad F. 2016. Superheated water extraction of glycyrrhizic acid from licorice root. Food Chem. 210, 396-401.

Shitu A, Izhar S, Tahir TM. 2015. Sub-critical water as a green solvent for production of valuable materials from agricultural waste biomass: A review of recent work. Global J. Environ. Sci. Manag. 1, 255-264.

Singanusong R, Nipornram S, Tochampa W, Rattanatraiwong P. 2015. Low power ultrasound-assisted extraction of phenolic compounds from mandarin (*Citrus reticulata* Blanco cv. Sainampueng) and lime (*Citrus aurantifolia*) peels and the antioxidant. Food Anal. Methods 8, 1112-1123.

Wang L, Wang J, Fang L, Zheng Z, Zhi D, Wang S, Li S, Ho CT, Zhao H. 2014. Anticancer activities of citrus peel polymethoxy flavones related to angiogenesis and others. Biomed Res. Int. 2014, 453972.

Yan Z, Zhang H, Sedem Dzah C, Zhang J, Diao C, Ma H, Duan Y. 2020. Subcritical water extraction, identification, antioxidant and antiproliferative activity of polyphenols from lotus seedpod. Sep. Purif. Technol. 236, 116217.

Ye Y, Chang X, Brennan MA, Brennan CS, Guo X. 2019. Comparison of phytochemical profiles, cellular antioxidant and anti-proliferative activities in five varieties of wampee (*Clausena lansium*) fruits. Int. J. Food Sci. Technol. 54,

2487-2493.

Yoon KN, Jang HS. 2018. Anti-xanthine oxidase, anti-cholinesterase, and anti-inflammatory activities of fruiting bodies of *Phellinus gilvus*. Korean J. Clin. Lab. Sci. 50, 225-235.

Yuan M, Liu Y, Xiao A, Leng J, Liao L, Ma L, Liu L. 2019. The interaction of dietary flavonoids with xanthine oxidase *in vitro*: Molecular property-binding affinity relationship aspects. RSC Adv. 9, 10781-10788.

Zhang H, Tian G, Zhao C, Han Y, DiMarco-Crook C, Lu C, Bao Y, Li C, Xiao H, Zheng J. 2019. Characterization of polymethoxyflavone demethylation during drying processes of citrus peels. Food Funct. 10, 5707-5717.

Publication List

Article

Kim DS, Lim SB. 2020. Standardization and Antioxidant Activity of Ethanol Extracts from Immature *Citrus unshiu* Pomace Antioxidants, In preparation.

Jamaludin R, **Kim DS**, Salleh LM, Lim SB. 2020. Kinetic study of subcritical water extraction of bioactive compounds from noni fruits. Ind. Crop. Prod., Under review.

Jamaludin R, **Kim DS**, Salleh LM, Lim SB. 2020. Optimization of high hydrostatic pressure extraction of bioactive compounds from noni fruits. J. Food Meas. Charact., Published online 02 July 2020.

Kim DS, Lim SB. 2020. Kinetic study of subcritical water extraction of bioflavonoids from *Citrus unshiu* peel. Sep. Purif. Technol. 250, 117259.

Kim DS, Lim SB. 2020. Semi-continuous subcritical water extraction of flavonoids from *Citrus unshiu* peel: their antioxidant and enzyme inhibitory activities. Antioxidants 9, 360.

Kim DS, Lim SB. 2019. Subcritical water extraction of rutin from the aerial parts of common buckwheat. J. Supercrit. Fluids 152(10), 104561.

Kim DS, Lim SB. 2018. Quality properties of subcritical water extracts of onion and onion juice product. J. Korean Soc. Food Sci. Nutr. 47(7), 750－758.

Kim DS, Lim SB. 2018. Composition of phenolic compounds and antioxidant activities if subcritical water extracts of onion skin. J. Korean Soc. Food Sci. Nutr. 47(4), 403－413.

Kim DS, Kim MB, Lim SB. 2017. Enhancement of phenolic production and antioxidant activity from buckwheat leaves by subcritical water extraction. Prev. Nutr. Food Sci. 22(4), 345－352.

Kim DS, Lim SB. 2017. Optimization of subcritical water hydrolysis of rutin into isoquercetin and quercetin. Prev. Nutr. Food Sci. 22(2), 131－137.

Ko JY, Ko MO, **Kim DS**, Lim SB. 2016. Enhanced production of phenolic compounds from pumpkin leaves by subcritical water hydrolysis. Prev. Nutr. Food Sci. 21(2), 132－137.

Patent

임상빈, **김동신**, 강경민. 이산화탄소를 첨가한 아임계수를 이용하여 양파껍질에서 분리되는 생리활성 성분을 증가시키는 방법. 대한민국 특허 등록번호 10-2054271, 등록일자 2019년12월04일.